

①

ARO Report 82 - 1

ADA 120945

**TRANSACTIONS OF THE TWENTY - SEVENTH
CONFERENCE OF ARMY MATHEMATICIANS**

**TERRAIN MICROROUGHNESS AND THE DYNAMIC
RESPONSE OF VEHICLES**

Richard A. Weiss

West Point, New York
June 1981



Approved for public release; distribution unlimited.
The findings in this report are not to be construed
as an official Department of the Army position, un-
less so designated by other authorized documents.

DTIC
ELECTE
S **D**
NOV 1 1982
B

DTIC FILE COPY

Sponsored by
The Army Mathematics Steering Committee
on behalf of
THE CHIEF OF RESEARCH, DEVELOPMENT
AND ACQUISITION

82 11 01 188

TERRAIN MICROROUGHNESS AND THE DYNAMIC RESPONSE OF VEHICLES

Richard A. Weiss
Mobility Systems Division
U. S. Army Engineer Waterways
Experiment Station, Vicksburg, MS 39180

ABSTRACT. The design of vehicles with particular operating characteristics on rough terrain requires accurate descriptors of terrain roughness. At present a one parameter description of surface roughness is available that uses the standard deviation of a detrended elevation profile. In order to introduce the frequency content of the terrain into the roughness description, a three parameter model of the surface roughness power spectrum is developed whose parameters are determined from the values of the standard deviation of displacement, slope and curvature obtained from a detrended elevation profile. The three parameter model predicts five distinct types of power spectra which can be used to classify terrain roughness including the cases where periodic features are present. For some types of terrain it is not necessary to use detrended data, and for these cases the power spectra are developed using an undetrended formalism.

The three parameter roughness model can be used to predict the power absorbed by the driver. The effects of vehicle geometry including wheel size, wheel spacing and track length are introduced in a natural way through the roughness model. Vehicle dynamics effects including the location of the driver relative to the center of mass of the vehicle are introduced by transmission functions. A comparison with experimental absorbed power data is made.

PART I: INTRODUCTION. The dynamic response of a specified type of wheeled vehicle operating on a terrain depends on the vehicle speed and the terrain roughness. For satisfactory operation of both vehicle and driver, the dynamic response of the vehicle must be predictable for a given type of terrain. To achieve this prediction capability, the U. S. Army Engineer Waterways Experiment Station (WES) was requested to develop improved methods of describing terrain and use them to calculate the resulting vehicle and driver motion.

A description of terrain roughness is especially important for the development of new vehicles because ride tests on various types of terrain are required to evaluate new design concepts. An accurate surface roughness description is required to separate the effects of a new vehicle design from the effects introduced by the surface roughness properties of a test site. Both the frequency content and the amplitude of an elevation profile will influence the ride quality of a vehicle, and an effect observed during a vehicle ride test may be due to a peculiarity of the terrain roughness rather than a specific vehicle effect.

The development of new vehicle designs is helped by a thorough understanding of how changes in the geometry and dynamics of a vehicle will interact with the terrain roughness to produce changes in the ride quality.

Especially important are the effects of geometry including wheel size, wheel spacing, driver location and track length, and the effects of dynamical parameters including spring constants, damping constants and the weight.¹ The effects of soil conditions are not treated although they may be important to the vehicle response.

Description of Terrain Roughness

A description of surface roughness begins with a measurement of an elevation profile, Figure 1a. Elevations are measured at small intervals (usually one foot or one half foot) over a distance of several hundred feet. Numerical differentiation gives the slope and curvature profiles. The measured elevations include gradual changes of elevation over a long distance. In some cases this nonstationary character of the measured elevation profile may have to be removed by a detrending procedure in order for the data to be processed. In other cases the measured elevation data can be used directly.

Roughness can be described as a stationary random process if the statistical properties of the profile height do not change with position along the profile. To remove nonstationary trends from the data a detrending procedure* is applied to the data which removes the very long wavelengths (the trend), see Figure 1b. The mathematical procedure for obtaining detrended data is given by²

$$F_d(x) = F(x) - \frac{1}{2\lambda} \int_0^{\infty} [F(x+a) + F(x-a)] e^{-a/\lambda} da \quad (1)$$

where $F_d(x)$ = detrended function

$F(x)$ = original function

λ = filter constant (detrending constant)

Computer program RRFN has been developed to calculate the detrended data from the original input data.¹

After removing the trend the question still remains as to the frequency constant of the terrain roughness. This is important because a dynamical system such as the spring support of a vehicle has a resonance frequency, and this resonance may be excited if the vehicle runs over a given terrain at a specified speed. Therefore it is of importance to know the wavelength content of the terrain roughness because this will determine the frequency content of the input displacement, velocity, and acceleration on the wheels of the moving vehicle. The wavelength content of a terrain displacement profile can be described by a power spectral density function.

The power spectral density (PSD) gives the spectral density of the variance of a random process.²⁻⁴ Therefore,

$$\sigma^2 = V = \int_0^{\infty} \text{PSD } d\Omega \quad (2)$$

* "Detrend" means to remove the trend of the elevation variations.

where σ = RMS value of the random process = standard deviation for zero average value

V = variance

Ω = spatial frequency = reciprocal wavelength = number of cycles/meter

In this paper the RMS value and the standard deviation will be used interchangeably because the baseline can be chosen so that all average values are zero. The PSD gives a measure of the frequency content of the random process. For example, the surface displacement profile PSD is a measure of the wavelength content of this profile.

One Parameter Model

A descriptor commonly used in terrain roughness models is the standard deviation (RMS) of displacement obtained from a measured elevation profile. The one parameter roughness power spectrum can be calculated from the value of the RMS displacement. The one parameter power spectra of the surface displacement and slope can be written as^{2,5}

$$P_d(\Omega) = \frac{C}{\Omega^2} \quad (3)$$

$$P_s(\Omega) = (2\pi)^2 \Omega^2 \left[\frac{\sin(\pi\Omega\Delta L)}{\pi\Omega\Delta L} \right]^2 P_d(\Omega) \quad (4)$$

where P_d = PSD of displacement profile

P_s = PSD of slope profile

C = roughness parameter

ΔL = interval of elevation of profile measurement

For the undetrended case the RMS displacement integral (2) does not converge with P_d given by equation (3), however the RMS slope integral (2) does converge with P_s given by equation (4). For the single parameter model a theoretical expression for the RMS value of the displacement can only be determined for detrended data, and the theoretical need for detrending is that it allows the elevation power spectrum integral to be evaluated. For this reason the value of the parameter C must be determined from detrended data. The spectral window function occurring in equation (4) introduces the interval of measurement of the elevation profile.

The power spectrum for a detrended elevation profile can be written as²

$$P_{d,DET}(\Omega, \lambda) = \frac{(2\pi\lambda)^4 \Omega^4}{[1 + (2\pi\lambda\Omega)^2]^2} P_d(\Omega) \quad (5)$$

$$= \phi^{-2} P_d(\Omega)$$

where the detrending function ϕ is defined by

$$\phi = 1 + (2\pi\lambda\Omega)^{-2} \quad (6)$$

Since the RMS integral of the slope power spectrum converges, Van Deusen uses the undetrended slope power spectrum given by equation (4) to calculate the RMS value of the slope. The integrals presented are²

$$\sigma_d^2 \text{ (Undetrended)} = \int_0^\infty P_d(\Omega) d\Omega \quad \text{Diverges} \quad (7)$$

$$\sigma_d^2 \text{ (Detrended, } \lambda) = \int_0^\infty P_{d, \text{DET}}(\Omega, \lambda) d\Omega = \frac{\pi^2 \lambda C}{2} \quad (8)$$

$$\sigma_s^2 \text{ (Undetrended)} = \int_0^\infty P_s(\Omega) d\Omega = \frac{2\pi^2 C}{\Delta L} \quad (9)$$

where σ_d = standard deviation of terrain displacement

σ_s = standard deviation of terrain slope

A determination of the RMS displacement for detrended data (by computer program RRFN, for example) immediately determines the constant C, and therefore the power spectrum for the undetrended data is calculated. Two basic theoretical concepts are introduced in the one parameter model: (a) the detrending function which allows the elevation RMS value to be calculated analytically, and (b) the slope spectral window function which introduces the measurement interval of the elevation profile. The value of σ_s can be used to calculate C directly from undetrended data using equation (9).^s

Three Parameter Model

A comparison of the one parameter monotonically decreasing power spectrum $P_d = C/\Omega^2$ with the power spectrum values obtained by calculating the Fourier transform of the autocorrelation function of an elevation profile suggests that the one parameter representation is valid only for high spatial frequencies of the terrain roughness. Also, quasi-random terrain areas such as plowed or disked agricultural fields cannot be described by a one parameter model because a pronounced peak occurs in the measured power spectrum at a frequency corresponding to the width of the plowed furrows.

A more complete description of surface roughness is needed, one that goes a step beyond a one parameter characterization that is based on a single RMS value of surface displacement. This paper introduces a three parameter roughness power spectrum model that can describe terrain areas having periodicities, and gives a better description of the roughness power spectrum in the long wavelength region.

The three power spectrum parameters are determined from the values of the standard deviations of the displacement, slope and curvature of a measured elevation profile (Figure 1a). The power spectrum determined by these parameters is found to be of five distinct types of which the Van Deusen form $C\Omega^{-2}$ is one. The displacement power spectrum $P_d(\Omega)$ is found to be a complicated function of frequency that includes spectral windows of definite bandwidth.

The resulting frequency channels of power transmission and power suppression may be responsible for the anomalous dynamic response of some vehicles on a given terrain.

Actual terrain locations where military trucks and track vehicles are expected to operate can vary considerably in quality (frequency) as well as their RMS values of elevation. Terrain types such as trails, cultivated fields, virgin terrain, test courses, etc., are expected to be encountered by military off-road vehicles. An attempt is made to classify terrain roughness in terms of the five basic types of roughness power spectra by associating each terrain site with one of the five types of power spectra. The type of power spectrum associated with a terrain site will determine the nature of the dynamic response of a vehicle moving over that terrain. In this way the expected dynamic response of a vehicle can be related to a specific terrain site. A computer program TERR was developed to accomplish this work.¹

Absorbed Power

Driver fatigue can be related to the power absorbed by a driver during the operation of a vehicle. Absorbed power is a physiological concept and by definition it is related to the acceleration power spectrum measured at the drivers seat.⁶ Experience has shown that a driver can absorb no more than six watts of power and be physically able to drive a vehicle for an extended period of time.⁷ It is of military interest to be able to predict the vehicle speed that corresponds to the six watt absorbed power level, and to determine the terrain roughness descriptors required to do this.

At present the six watt speed is estimated from the RMS value of surface displacement as determined from a detrended elevation profile.⁸⁻¹³ This single parameter terrain roughness description is sometimes found to be inadequate because the frequency content of the ground surface elevation is not considered. The three parameter terrain roughness description was developed in part to improve the method of determining the six watt speed by including the effects of frequency content.



Accession For	
NTIS GRA&I	<input checked="checked" type="checkbox"/>
DTIC TAB	<input type="checkbox"/>
Unannounced	<input type="checkbox"/>
Justification	
By	
Distribution/	
Availability Codes	
Dist	Avail and/or Special
A	

PART II: THEORETICAL ROUGHNESS MODELS

INTRODUCTORY REMARKS. Terrain areas can be natural or man-made or a combination of both types. Natural terrain elevations appear to be random, but some features such as windblown sand dunes have an apparent regularity. Man-made areas such as roads, trails, plowed and disked fields, etc., can contain apparent regularities although their elevation profiles are still characterized as random data. Plowed fields, for example, exhibit a quasi-sinusoidal pattern and will have a power spectrum that peaks at a spatial frequency that corresponds to the quasi-sinusoidal pattern. This case clearly cannot be described by a one parameter power spectrum of the form $C\Omega^{-2}$ which is a monotonically decreasing function of spatial frequency. This part of the paper develops a three parameter power spectrum model that can be used to describe random terrain roughness elevation which include regularities, man-made or natural.

The power spectrum coefficients of the three parameter model are calculated from the RMS values of elevation, slope and curvature that are obtained from a detrended elevation profile or from an undetrended elevation profile when possible. The values of these three parameters can be used to classify terrain roughness.

FORM OF THE THREE PARAMETER POWER SPECTRUM. This section suggests an appropriate form for the three parameter roughness power spectrum. The choice of the form of the three parameter power spectrum model is a natural extension of the Van Deusen one parameter model $C\Omega^{-2}$. Figure 2a shows that the PSD of the undetrended and detrended displacement profile is described by the form $C\Omega^{-2}$ only in the region of large Ω (short wavelengths). For small Ω (long wavelength) the PSD deviates from that predicted by $C\Omega^{-2}$. Additional parameters are required to describe the deviation from $C\Omega^{-2}$ in the region of small Ω . Assuming that the short wavelength region is accurately described by the form $C\Omega^{-2}$, the modification of the PSD must consist of terms $\Omega^{-\alpha}$ (with $\alpha > 2$) that are added to the $C\Omega^{-2}$ term. In this way the modification of the PSD becomes important only for small Ω and approaches the form $C\Omega^{-2}$ for large Ω .

The PSD for undetrended surface displacement can be written as a generalization of $C\Omega^{-2}$ in the form of a power series as follows

$$P_d = C\Omega^{-2} + D\Omega^{-3} + E\Omega^{-4} + \dots \quad (10)$$

For practical calculation, the power series must be cut off at some finite term. If two parameters are chosen to describe P_d in the form

$$P_d = C\Omega^{-2} + D\Omega^{-3} \quad (11)$$

then the measurement of both σ_d and σ_s is required to determine C and D. If three parameters are chosen to describe P_d in the form

$$P_d = C\Omega^{-2} + D\Omega^{-3} + E\Omega^{-4} \quad (12)$$

then σ_d , σ_s and σ_c would be required to determine C, D, and E, where σ_c = standard deviation of curvature (second derivative of elevation with regard to space coordinate). In this paper the term curvature will be used to describe the second derivative.

Polynomial models beginning with the term $A\Omega^{-1}$ such as

$$P_d = A\Omega^{-1} + C\Omega^{-2} + D\Omega^{-3} \quad (13)$$

are not valid for two reasons: (1) they do not approach the Van Deusen form $C\Omega^{-2}$ for large Ω , and (2) the integral $\int_0^\infty P_d \phi^{-2} d\Omega$ for detrended data has a logarithmic singularity and cannot be evaluated.

The short wavelength (high frequency) part of the power spectrum is described by the parameter C, while the long wavelength (low frequency) part of the power spectrum is described by the parameter E. The middle ranges of frequency are determined by the parameter D. The values of the power spectrum parameters C, D and E are determined by the type of terrain elevation profile that is measured, and these parameters can be used as descriptive numbers to classify terrain roughness.

CLASSIFICATION OF TERRAIN ROUGHNESS. This section shows how a terrain roughness classification can be developed in a natural way from the algebraic signs of the parameters C, D and E. Terrain roughness can be classified according to the shape of the power spectrum associated with the natural elevation profile. The shape of a theoretically predicted roughness power spectrum is determined by the values of the parameters C, D and E. These parameters will be determined from the values of σ_d , σ_s and σ_c associated with the elevation profile.

A priori, the values of the three parameters can be positive or negative yielding a total of $2 \times 2 \times 2 = 8$ possible types of power spectra. But the case $C < 0$, $D < 0$ and $E < 0$ must obviously be excluded because the power spectrum must be positive at least in some frequency range. This leaves seven possibilities. But of these seven cases two are redundant and only five physically distinct types of elevation power spectra are possible for the three parameter model. These are shown in Figure 2b. The basic forms of Type 2 and Type 3 remain unchanged for $D > 0$ or $D < 0$ so that either sign still represents only one spectral type, and this redundancy yields only five distinct spectral classes.

The one parameter power spectrum $C\Omega^{-2}$ is seen to be a special case of a Type 1 power spectrum with $C > 0$, $D = 0$ and $E = 0$. Type 1 power spectrum contains all frequencies with little power at the high frequencies. Type 2 has no power at high frequencies. Types 3 and 4 have pronounced peaks at definite

frequencies and can be used to describe a large scale rolling type of terrain. Type 4 with $D^2 < 4CE$ gives a power spectrum which is all negative and so this case must be excluded. Type 5B with $D^2 > 4CE$ describes the situation where a high frequency periodicity occurs within the terrain, such as in the case of plowed or disked fields. Type 5A with $D^2 < 4CE$ can be considered to be a special case of Type 1 where the power is positive for all frequencies.

Power spectra, by definition as the Fourier transform of an autocorrelation, are always positive. Therefore only the frequency ranges where $P_d(\Omega)$ is positive in Figure 2b are physically acceptable. The regions where $P_d(\Omega)$ become negative must be regarded as physically unacceptable for power transmission and $P_d(\Omega)$ is set equal to zero here. In this manner it is seen that the roughness power spectrum $P_d(\Omega)$ is not in general a simple function but rather may contain cutoff frequencies (Ω_0 and Ω_1) which produce "windows" (bright areas) and zero power areas (dark regions) of definite bandwidths. Therefore only in distinct frequency regions may power be transferred to a moving vehicle. The type of power spectrum exhibited by a given site is determined from measured values of σ_d , σ_s and σ_c from which the values of C, D and E are obtained.

The power spectra used are one-sided because they are defined only for positive frequencies. Sometimes two-sided power spectra are used which are defined for positive and negative frequencies. The two-sided power spectra can be obtained as mirror images of the one-sided power spectra. Power spectra must be symmetrical about the zero frequency axis because they are defined as Fourier transforms of autocorrelation functions which themselves are symmetrical. The power spectrum model given in (12) can be used for negative Ω by choosing $|\Omega|^3$, absolute value of Ω , in the regions of negative Ω .

The type of power spectrum obtained from an elevation profile will depend on the length of the measured profile. Therefore the classification of terrain areas will be scale dependent, and a comparison of two terrain areas should be made on the basis of equal elevation profile lengths. This paper does not investigate scale dependence.

The five possible types of roughness power spectra are associated with the choice of a three parameter power spectrum model. The choice of a greater number of parameters would produce more complicated power spectrum shapes. For example a four parameter model would exhibit two additional types of spectra giving a total of seven types. The three parameter choice made in this paper is justified by noting that Newton's law of motion relates the force acting on a vehicle to the acceleration input. Therefore as far as vehicle dynamics is concerned there are three stochastic kinematic quantities to be obtained: acceleration, velocity and displacement. This suggests a three parameter surface roughness model because the standard deviations of velocity σ_v and acceleration σ_a can be related to the standard deviations of the slope σ_s and curvature σ_c , respectively, of the terrain elevation profile (Part III). Therefore the calculation of the basic kinematic quantities associated with the vertical dynamic response of vehicles (σ_d , σ_v , σ_a) requires the three measured

roughness quantities σ_d , σ_s and σ_c from which three power spectrum parameters (C, D and E) can be determined.

THREE PARAMETER MODEL OF DETRENDED TERRAIN ROUGHNESS DATA. This section develops the formalism and mathematical details required to evaluate the power spectrum of a measured elevation profile from the RMS values of the elevation, slope and curvature obtained from the corresponding detrended elevation profile. This is done for each of the five types of power spectra described above.

For roughness power spectra of Types 1, 2 and 5 it is impossible to use values of σ_d , σ_s and σ_c obtained directly from undetrended data to calculate the power spectrum coefficients because the integral $\int_0^\infty P_d d\Omega$ diverges (at $\Omega = 0$) for the form of power spectrum given in equation (12). These three types of terrain roughness must be handled using detrended data and the values of σ_d , σ_s and σ_c for detrended data can be related to integrals of the form $\int_0^\infty P_d \phi^{-2} d\Omega$ which converges. For roughness spectra of Types 3 and 4 it is not necessary to use detrended data because the integrals defining σ_d , σ_s and σ_c are defined from a lower cutoff frequency Ω_0 and so the singularity at $\Omega = 0$ is avoided and undetrended data can be used. But the detrended formalism can be applied to spectra of Types 3 and 4, and this section evaluates the integrals that appear in the mathematical expressions for σ_d , σ_s and σ_c (for detrended data) for all five types of terrain roughness power spectra.

For the power spectrum given by equation (12), the values of P_d , P_s and P_c for undetrended data are

$$P_d = C\Omega^{-2} + D\Omega^{-3} + E\Omega^{-4} \quad (14)$$

$$P_s = (2\pi)^2 \Omega^2 (C\Omega^{-2} + D\Omega^{-3} + E\Omega^{-4}) \left[\frac{\sin(\pi\Omega\Delta L)}{\pi\Omega\Delta L} \right]^2 \quad (15)$$

$$P_c = (2\pi)^4 \Omega^4 (C\Omega^{-2} + D\Omega^{-3} + E\Omega^{-4}) \left[\frac{\sin(\pi\Omega\Delta L)}{\pi\Omega\Delta L} \right]^4 \quad (16)$$

The form for the slope and curvature PSD is developed in Reference 1.

The necessary integrals for the detrended scheme of the three parameter model will now be evaluated. This will be done for each of the five basic types of roughness power spectrum.

Type 1 Power Spectrum

The variance integrals of P_d and P_s cannot be performed directly on (14) and (15) because they are singular for $\Omega = 0$. In order to calculate C, D and E, the variance of the detrended displacement, slope and curvature profiles must be used. For the case of detrended data the displacement, slope and

curvature power spectral densities are $P_d \phi^{-2}$, $P_s \phi^{-2}$ and $P_c \phi^{-2}$ respectively where ϕ is defined by (7). From (14) - (16) the RMS values of the detrended terrain displacement, slope and curvature are

$$\sigma_d^2 = V_d = \int_0^\infty P_d \phi^{-2} d\Omega = C f_1(\lambda) + D f_2(\lambda) + E f_3(\lambda) \quad (17)$$

$$\sigma_s^2 = V_s = \int_0^\infty P_s \phi^{-2} d\Omega = C g_1(\lambda) + D g_2(\lambda) + E g_3(\lambda) \quad (18)$$

$$\sigma_c^2 = V_c = \int_0^\infty P_c \phi^{-2} d\Omega = C h_1(\lambda) + D h_2(\lambda) + E h_3(\lambda) \quad (19)$$

The values of σ_d^2 , σ_s^2 and σ_c^2 are represented as a linear combination of integrals where the $f_i(\lambda)$, $g_i(\lambda)$ and $h_i(\lambda)$ are given, with $b = 2\pi\lambda$ and $a = \pi\Delta L$, as

$$f_1(\lambda) = \int_0^\infty \Omega^{-2} \phi^{-2} d\Omega = b^4 \int_0^\infty \frac{\Omega^2 d\Omega}{(1 + b^2 \Omega^2)^2} \quad (20)$$

$$f_2(\lambda) = \int_0^\infty \Omega^{-3} \phi^{-2} d\Omega = b^4 \int_0^\infty \frac{\Omega d\Omega}{(1 + b^2 \Omega^2)^2} \quad (21)$$

$$f_3(\lambda) = \int_0^\infty \Omega^{-4} \phi^{-2} d\Omega = b^4 \int_0^\infty \frac{d\Omega}{(1 + b^2 \Omega^2)^2} \quad (22)$$

$$g_1(\lambda) = (2\pi)^2 \int_0^\infty \left(\frac{\sin a\Omega}{a\Omega} \right)^2 \phi^{-2} d\Omega = \frac{(2\pi)^2 b^4}{a^2} \int_0^\infty \frac{\Omega^2 \sin^2(a\Omega) d\Omega}{(1 + b^2 \Omega^2)^2} \quad (23)$$

$$g_2(\lambda) = (2\pi)^2 \int_0^\infty \Omega^{-1} \left(\frac{\sin a\Omega}{a\Omega} \right)^2 \phi^{-2} d\Omega = \frac{(2\pi)^2 b^4}{a^2} \int_0^\infty \frac{\Omega \sin^2(a\Omega) d\Omega}{(1 + b^2 \Omega^2)^2} \quad (24)$$

$$g_3(\lambda) = (2\pi)^2 \int_0^\infty \Omega^{-2} \left(\frac{\sin a\Omega}{a\Omega} \right)^2 \phi^{-2} d\Omega = \frac{(2\pi)^2 b^4}{a^2} \int_0^\infty \frac{\sin^2(a\Omega) d\Omega}{(1 + b^2 \Omega^2)^2} \quad (25)$$

$$h_1(\lambda) = (2\pi)^4 \int_0^\infty \Omega^2 \left(\frac{\sin a\Omega}{a\Omega} \right)^4 \phi^{-2} d\Omega = \frac{(2\pi)^4 b^4}{a^4} \int_0^\infty \frac{\Omega^2 \sin^4(a\Omega) d\Omega}{(1 + b^2 \Omega^2)^2} \quad (26)$$

$$h_2(\lambda) = (2\pi)^4 \int_0^\infty \Omega \left(\frac{\sin a\Omega}{a\Omega} \right)^4 \phi^{-2} d\Omega = \frac{(2\pi)^4 b^4}{a^4} \int_0^\infty \frac{\Omega \sin^4(a\Omega) d\Omega}{(1 + b^2 \Omega^2)^2} \quad (27)$$

$$h_3(\lambda) = (2\pi)^4 \int_0^\infty \left(\frac{\sin a\Omega}{a\Omega} \right)^4 \phi^{-2} d\Omega = \frac{(2\pi)^4 b^4}{a^4} \int_0^\infty \frac{\sin^4(a\Omega) d\Omega}{(1 + b^2 \Omega^2)^2} \quad (28)$$

Note the integrals g_1 , g_2 , h_1 , h_2 and h_3 diverge where $a = 0$, so that σ_s and σ_c diverge for $\Delta L = 0$. Only for the case $\Delta L \neq 0$ are σ_d , σ_s and σ_c properly defined by infinite integrals when $\Omega \rightarrow \infty$. Also, the integrals representing σ_d and σ_s would diverge in the low frequency limit if the detrending factor ϕ^{-2} were not inserted into these integrals. In other words, whereas $\Delta L \neq 0$ avoids singularities at high frequencies, the detrending factor ϕ^{-2} avoids singularities at low frequencies.

The values of the integrals in (20) - (28) are evaluated in Reference 1 by complex integration using the contours shown in Figure 2c, and have the following values

$$f_1(\lambda) = \frac{\pi b}{4} \quad (29)$$

$$f_2(\lambda) = \frac{b^2}{2} \quad (30)$$

$$f_3(\lambda) = \frac{\pi b^3}{4} \quad (31)$$

$$g_1(\lambda) = \frac{\pi^3 b}{a^2} \left[\frac{1}{2} \left(1 - e^{-2a/b} \right) + \frac{a}{b} e^{-2a/b} \right] \quad (32)$$

$$g_2(\lambda) = \frac{\pi^2 b}{a^2} \left[e^{2a/b} E_1(2a/b) + e^{-2a/b} E^*(2a/b) \right] \quad (33)$$

$$g_3(\lambda) = \frac{\pi^3 b^3}{a^2} \left[\frac{1}{2} \left(1 - e^{-2a/b} \right) - \frac{a}{b} e^{-2a/b} \right] \quad (34)$$

$$h_1(\lambda) = \frac{4\pi^5 b}{a^4} \left[\frac{3}{8} + \frac{e^{-4a/b}}{8} - \frac{e^{-2a/b}}{2} + \frac{a}{b} e^{-2a/b} \left(1 - \frac{1}{2} e^{-2a/b} \right) \right] \quad (35)$$

$$h_2(\lambda) = \frac{4\pi^4 b}{a^3} \left\{ e^{2a/b} E_1(2a/b) + e^{-2a/b} E^*(2a/b) - \frac{1}{2} \left[e^{4a/b} E_1(4a/b) + e^{-4a/b} E^*(4a/b) \right] \right\} \quad (36)$$

$$h_3(\lambda) = \frac{4\pi^5 b^3}{a^4} \left[\frac{3}{8} - \frac{1}{2} e^{-2a/b} \left(1 - \frac{1}{4} e^{-2a/b} \right) - \frac{a}{b} e^{-2a/b} \left(1 - \frac{1}{2} e^{-2a/b} \right) \right] \quad (37)$$

where $E_1(x)$ and $E^*(x)$ are exponential integral functions which are tabulated in the literature. The exponential integrals are defined as follows

$$E_1(x) = -\text{Ei}(-x) = \int_x^\infty \frac{e^{-t}}{t} dt \quad (38)$$

$$E^*(x) = \text{Ei}(x) = \int_{-\infty}^x \frac{e^t}{t} dt \quad (39)$$

For small values of x these functions have the following series expansions

$$E_1(x) = -\gamma - \log_e(x) + x - \frac{x^2}{2!2} + \frac{x^3}{3!3} - \frac{x^4}{4!4} + \frac{x^5}{5!5} - \dots \quad (40)$$

$$E^*(x) = \gamma + \log_e(x) + x + \frac{x^2}{2!2} + \frac{x^3}{3!3} + \frac{x^4}{4!4} + \frac{x^5}{5!5} + \dots \quad (41)$$

where γ = Euler constant = 0.5772157.

Type 2 Roughness Spectrum

Detrended data must be used for this case. The integrals defining V_d , V_s and V_c are (see Figure 2b)

$$\sigma_d^2 = \int_0^{\Omega_0} P_d \phi^{-2} d\Omega = C\Delta f_1(\lambda, \Omega_0) + D\Delta f_2(\lambda, \Omega_0) + E\Delta f_3(\lambda, \Omega_0) \quad (42)$$

$$\sigma_s^2 = \int_0^{\Omega_0} P_s \phi^{-2} d\Omega = C\Delta g_1(\lambda, \Omega_0) + D\Delta g_2(\lambda, \Omega_0) + E\Delta g_3(\lambda, \Omega_0) \quad (43)$$

$$\sigma_c^2 = \int_0^{\Omega_0} P_c \phi^{-2} d\Omega = C\Delta h_1(\lambda, \Omega_0) + D\Delta h_2(\lambda, \Omega_0) + E\Delta h_3(\lambda, \Omega_0) \quad (44)$$

where the integrals $\Delta f_j(\lambda, \Omega_0)$, $\Delta g_j(\lambda, \Omega_0)$ and $\Delta h_j(\lambda, \Omega_0)$ are given by

$$\Delta f_1(\lambda, \Omega_0) = b^4 \int_0^{\Omega_0} \frac{\Omega^2 d\Omega}{(1 + b^2 \Omega^2)^2} = \frac{b}{2} (\theta_0 - \sin \theta_0 \cos \theta_0) \sim \frac{b^4 \Omega_0^3}{3} \quad (45)$$

$$\Delta f_2(\lambda, \Omega_0) = b^4 \int_0^{\Omega_0} \frac{\Omega d\Omega}{(1 + b^2 \Omega^2)^2} = \frac{b^2}{2} \sin^2 \theta_0 \sim \frac{b^4 \Omega_0^2}{2} \quad (46)$$

$$\Delta f_3(\lambda, \Omega_0) = b^4 \int_0^{\Omega_0} \frac{d\Omega}{(1 + b^2 \Omega^2)^2} \approx \frac{b^3}{2} (\theta_0 + \sin \theta_0 \cos \theta_0) \sim b^4 \Omega_0 \quad (47)$$

where

$$\theta_0 = \tan^{-1}(b\Omega_0) \quad (48)$$

$$\begin{aligned} \Delta g_1(\lambda, \Omega_0) &= \left(\frac{2\pi}{a}\right)^2 b^4 \int_0^{\Omega_0} \frac{\Omega^2 \sin^2(a\Omega) d\Omega}{(1 + b^2 \Omega^2)^2} \\ &= \frac{1}{2} \left(\frac{2\pi}{a}\right)^2 b^4 \left[L_0(\Omega_0) - L_1^{(2a)}(\Omega_0) + L_2^{(2a)}(\Omega_0) - \dots \right] \end{aligned} \quad (49)$$

where

$$L_0(\Omega_0) = \Omega_0^3 \left(\frac{1}{3} - \frac{2}{5} b^2 \Omega_0^2 + \frac{3}{7} b^4 \Omega_0^4 - \frac{4}{9} b^6 \Omega_0^6 + \frac{5}{11} b^8 \Omega_0^8 - \dots \right)$$

$$L_1^{(2a)}(\Omega_0) = \frac{\Omega_0^2 \sin(2a\Omega_0)}{2a} + \frac{2\Omega_0 \cos(2a\Omega_0)}{(2a)^2} - \frac{2 \sin(2a\Omega_0)}{(2a)^3}$$

$$\begin{aligned} L_2^{(2a)}(\Omega_0) &= 2b^2 \left\{ \left[4(2a)^2 \Omega_0^2 - 24 \right] \frac{\Omega_0 \cos(2a\Omega_0)}{(2a)^4} \right. \\ &\quad \left. + \left[(2a)^4 \Omega_0^4 - 12(2a)^2 \Omega_0^2 + 24 \right] \frac{\sin(2a\Omega_0)}{(2a)^5} \right\} \end{aligned}$$

$$\begin{aligned} \Delta g_2(\lambda, \Omega_0) &= \left(\frac{2\pi}{a}\right)^2 b^4 \int_0^{\Omega_0} \frac{\Omega \sin^2(a\Omega) d\Omega}{(1 + b^2 \Omega^2)^2} \\ &= \frac{1}{2} \left(\frac{2\pi}{a}\right)^2 b^4 \left[W_0(\Omega_0) - W_1^{(2a)}(\Omega_0) + W_2^{(2a)}(\Omega_0) - \dots \right] \end{aligned} \quad (50)$$

where

$$w_0(\Omega_0) = \frac{\Omega_0^2}{2} (1 - b^2 \Omega_0^2 + b^4 \Omega_0^4 - b^6 \Omega_0^6 + b^8 \Omega_0^8 - \dots)$$

$$w_1^{(2a)}(\Omega_0) = \frac{\Omega_0 \sin(2a\Omega_0)}{2a} + \frac{\cos(2a\Omega_0)}{(2a)^2} - \frac{1}{(2a)^2}$$

$$w_2^{(2a)}(\Omega_0) = 2b^2 \left\{ \left[\frac{3\Omega_0^2}{(2a)^2} - \frac{6}{(2a)^4} \right] \cos(2a\Omega_0) + \frac{6}{(2a)^4} + \left[\frac{\Omega_0^2}{2a} - \frac{6}{(2a)^3} \right] \Omega_0 \sin(2a\Omega_0) \right\}$$

$$\begin{aligned} \Delta g_3(\lambda, \Omega_0) &= \left(\frac{2\pi}{a} \right)^2 b^4 \int_0^{\Omega_0} \frac{\sin^2(a\Omega) d\Omega}{(1 + b^2 \Omega^2)^2} \\ &= \frac{1}{2} \left(\frac{2\pi}{a} \right)^2 b^4 \left[H_0(\Omega_0) - H_1^{(2a)}(\Omega_0) + H_2^{(2a)}(\Omega_0) - \dots \right] \end{aligned} \quad (51)$$

where

$$H_0(\Omega_0) = \Omega_0 \left(1 - \frac{2}{3} b^2 \Omega_0^2 + \frac{3}{5} b^4 \Omega_0^4 - \frac{4}{7} b^6 \Omega_0^6 + \frac{5}{9} b^8 \Omega_0^8 - \dots \right)$$

$$H_1^{(2a)}(\Omega_0) = \frac{\sin(2a\Omega_0)}{2a}$$

$$H_2^{(2a)}(\Omega_0) = 2b^2 \left[\frac{\Omega_0^2 \sin(2a\Omega_0)}{2a} + \frac{2\Omega_0 \cos(2a\Omega_0)}{(2a)^2} - \frac{2 \sin(2a\Omega_0)}{(2a)^3} \right]$$

$$\begin{aligned}
\Delta h_1(\lambda, \Omega_0) &= \left(\frac{2\pi}{a}\right)^4 b^4 \int_0^{\Omega_0} \frac{\Omega^2 \sin^4(a\Omega) d\Omega}{(1 + b^2 \Omega^2)^2} \\
&= \frac{1}{4} \left(\frac{2\pi}{a}\right)^4 b^4 \left\{ \frac{3}{2} L_0(\Omega_0) - 2 \left[L_1^{(2a)}(\Omega_0) - L_2^{(2a)}(\Omega_0) + \dots \right] \right. \\
&\quad \left. + \frac{1}{2} \left[L_1^{(4a)}(\Omega_0) - L_2^{(4a)}(\Omega_0) + L_3^{(4a)}(\Omega_0) - \dots \right] \right\}
\end{aligned} \tag{52}$$

where

$$L_1^{(4a)}(\Omega_0) = \frac{\Omega_0^2 \sin(4a\Omega_0)}{4a} + \frac{2\Omega_0 \cos(4a\Omega_0)}{(4a)^2} - \frac{2 \sin(4a\Omega_0)}{(4a)^3}$$

$$\begin{aligned}
L_2^{(4a)}(\Omega_0) &= 2b^2 \left\{ \left[4(4a)^2 \Omega_0^2 - 24 \right] \frac{\Omega_0 \cos(4a\Omega_0)}{(4a)^4} \right. \\
&\quad \left. + \left[(4a)^4 \Omega_0^4 - 12(4a)^2 \Omega_0^2 + 24 \right] \frac{\sin(4a\Omega_0)}{(4a)^5} \right\}
\end{aligned}$$

$$\begin{aligned}
\Delta h_2(\lambda, \Omega_0) &= \left(\frac{2\pi}{a}\right)^4 b^4 \int_0^{\Omega_0} \frac{\Omega \sin^4(a\Omega) d\Omega}{(1 + b^2 \Omega^2)^2} \\
&= \frac{1}{4} \left(\frac{2\pi}{a}\right)^4 b^4 \left\{ \frac{3}{2} W_0(\Omega_0) - 2 \left[W_1^{(2a)}(\Omega_0) - W_2^{(2a)}(\Omega_0) + \dots \right] \right. \\
&\quad \left. + \frac{1}{2} \left[W_1^{(4a)}(\Omega_0) - W_2^{(4a)}(\Omega_0) + \dots \right] \right\}
\end{aligned} \tag{53}$$

where

$$W_1^{(4a)}(\Omega_0) = \frac{\Omega_0 \sin(4a\Omega_0)}{4a} + \frac{\cos(4a\Omega_0)}{(4a)^2} - \frac{1}{(4a)^2}$$

$$w_2^{(4a)}(\Omega_0) = 2b^2 \left\{ \left[\frac{3\Omega_0^2}{(4a)^2} - \frac{6}{(4a)^4} \right] \cos(4a\Omega_0) + \frac{6}{(4a)^4} + \left[\frac{\Omega_0^2}{4a} - \frac{6}{(4a)^3} \right] \Omega_0 \sin(4a\Omega_0) \right\}$$

$$\begin{aligned} \Delta h_3(\lambda, \Omega_0) &= \left(\frac{2\pi}{a} \right)^4 b^4 \int_0^{\Omega_0} \frac{\sin^4(a\Omega) d\Omega}{(1 + b^2\Omega^2)^2} \\ &= \frac{1}{4} \left(\frac{2\pi}{a} \right)^4 b^4 \left\{ \frac{3}{2} H_0(\Omega_0) - 2 \left[H_1^{(2a)}(\Omega_0) - H_2^{(2a)}(\Omega_0) + \dots \right] \right. \\ &\quad \left. + \frac{1}{2} \left[H_1^{(4a)}(\Omega_0) - H_2^{(4a)}(\Omega_0) + \dots \right] \right\} \end{aligned} \quad (54)$$

where

$$H_1^{(4a)}(\Omega_0) = \frac{\sin(4a\Omega_0)}{4a}$$

$$H_2^{(4a)}(\Omega_0) = 2b^2 \left[\frac{\Omega_0^2 \sin(4a\Omega_0)}{4a} + \frac{2\Omega_0 \cos(4a\Omega_0)}{(4a)^2} - \frac{2 \sin(4a\Omega_0)}{(4a)^3} \right]$$

Type 3 Roughness Spectrum

Either the detrended or undetrended procedure can be used for this case. The integrals defining V_d , V_s and V_c for the detrended case are (see Figure 2b)

$$\sigma_d^2 = \int_{\Omega_0}^{\infty} P_d \phi^{-2} d\Omega = C f_1(\lambda, \Omega_0) + D f_2(\lambda, \Omega_0) + E f_3(\lambda, \Omega_0) \quad (55)$$

$$\sigma_s^2 = \int_{\Omega_0}^{\infty} P_s \phi^{-2} d\Omega = C g_1(\lambda, \Omega_0) + D g_2(\lambda, \Omega_0) + E g_3(\lambda, \Omega_0) \quad (56)$$

$$\sigma_c^2 = \int_{\Omega_0}^{\infty} P_c \phi^{-2} d\Omega = C h_1(\lambda, \Omega_0) + D h_2(\lambda, \Omega_0) + E h_3(\lambda, \Omega_0) \quad (57)$$

The integrals $f_j(\lambda, \Omega_0)$, $g_j(\lambda, \Omega_0)$ and $h_j(\lambda, \Omega_0)$ are given by

$$f_j(\lambda, \Omega_0) = b^4 \int_{\Omega_0}^{\infty} \frac{\Omega^{3-j} d\Omega}{(1 + b^2 \Omega^2)^2} = f_j(\lambda) - \Delta f_j(\lambda, \Omega_0) \quad (58)$$

$$g_j(\lambda, \Omega_0) = \left(\frac{2\pi}{a}\right)^2 b^4 \int_{\Omega_0}^{\infty} \frac{\Omega^{3-j} \sin^2(a\Omega) d\Omega}{(1 + b^2 \Omega^2)^2} = g_j(\lambda) - \Delta g_j(\lambda, \Omega_0) \quad (59)$$

$$h_j(\lambda, \Omega_0) = \left(\frac{2\pi}{a}\right)^4 b^4 \int_{\Omega_0}^{\infty} \frac{\Omega^{3-j} \sin^4(a\Omega) d\Omega}{(1 + b^2 \Omega^2)^2} = h_j(\lambda) - \Delta h_j(\lambda, \Omega_0) \quad (60)$$

Type 4 Power Spectrum

Either the detrended or undetrended scheme can be used for this case. The integrals defining V_d , V_s and V_c for this case are (see Figure 2b)

$$\sigma_d^2 = \int_{\Omega_0}^{\Omega_1} P_d \phi^{-2} d\Omega = C f_1(\lambda, \Omega_0, \Omega_1) + D f_2(\lambda, \Omega_0, \Omega_1) + E f_3(\lambda, \Omega_0, \Omega_1) \quad (61)$$

$$\sigma_s^2 = \int_{\Omega_0}^{\Omega_1} P_s \phi^{-2} d\Omega = C g_1(\lambda, \Omega_0, \Omega_1) + D g_2(\lambda, \Omega_0, \Omega_1) + E g_3(\lambda, \Omega_0, \Omega_1) \quad (62)$$

$$\sigma_c^2 = \int_{\Omega_0}^{\Omega_1} P_c \phi^{-2} d\Omega = Ch_1(\lambda, \Omega_0, \Omega_1) + Dh_2(\lambda, \Omega_0, \Omega_1) + Eh_3(\lambda, \Omega_0, \Omega_1) \quad (63)$$

The integrals $f_j(\lambda, \Omega_0, \Omega_1)$, $g_j(\lambda, \Omega_0, \Omega_1)$, and $h_j(\lambda, \Omega_0, \Omega_1)$ are given by

$$f_j(\lambda, \Omega_0, \Omega_1) = b^4 \int_{\Omega_0}^{\Omega_1} \frac{\Omega^{3-j} d\Omega}{(1 + b^2 \Omega^2)^2} = \Delta f_j(\lambda, \Omega_1) - \Delta f_j(\lambda, \Omega_0) \quad (64)$$

$$g_j(\lambda, \Omega_0, \Omega_1) = \left(\frac{2\pi}{a}\right)^2 b^4 \int_{\Omega_0}^{\Omega_1} \frac{\Omega^{3-j} \sin^2 \left(\frac{a\Omega}{2}\right) d\Omega}{(1 + b^2 \Omega^2)^2} = \Delta g_j(\lambda, \Omega_1) - \Delta g_j(\lambda, \Omega_0) \quad (65)$$

$$h_j(\lambda, \Omega_0, \Omega_1) = \left(\frac{2\pi}{a}\right)^4 b^4 \int_{\Omega_0}^{\Omega_1} \frac{\Omega^{3-j} \sin^4 \left(\frac{a\Omega}{2}\right) d\Omega}{(1 + b^2 \Omega^2)^2} = \Delta h_j(\lambda, \Omega_1) - \Delta h_j(\lambda, \Omega_0) \quad (66)$$

Type 5B Power Spectrum

The detrended scheme must be used for this case. The integrals defining V_d , V_s and V_c are (see Figure 2b)

$$\begin{aligned} \sigma_d^2 &= \int_0^{\Omega_0} P_d \phi^{-2} d\Omega + \int_{\Omega_1}^{\infty} P_d \phi^{-2} d\Omega \\ &= C\delta f_1(\lambda, \Omega_0, \Omega_1) + D\delta f_2(\lambda, \Omega_0, \Omega_1) + E\delta f_3(\lambda, \Omega_0, \Omega_1) \end{aligned} \quad (67)$$

$$\sigma_s^2 = \int_0^{\Omega_0} P_s \phi^{-2} d\Omega + \int_{\Omega_1}^{\infty} P_s \phi^{-2} d\Omega \quad (68)$$

$$= C\delta g_1(\lambda, \Omega_0, \Omega_1) + D\delta g_2(\lambda, \Omega_0, \Omega_1) + E\delta g_3(\lambda, \Omega_0, \Omega_1)$$

$$\sigma_c^2 = \int_0^{\Omega_0} P_c \phi^{-2} d\Omega + \int_{\Omega_1}^{\infty} P_c \phi^{-2} d\Omega \quad (69)$$

$$= C\delta h_1(\lambda, \Omega_0, \Omega_1) + D\delta h_2(\lambda, \Omega_0, \Omega_1) + E\delta h_3(\lambda, \Omega_0, \Omega_1)$$

The integrals $\delta f_j(\lambda, \Omega_0, \Omega_1)$, $\delta g_j(\lambda, \Omega_0, \Omega_1)$ and $\delta h_j(\lambda, \Omega_0, \Omega_1)$ are given by

$$\delta f_j(\lambda, \Omega_0, \Omega_1) = \Delta f_j(\lambda, \Omega_0) + f_j(\lambda, \Omega_1) = f_j(\lambda) + \Delta f_j(\lambda, \Omega_0) - \Delta f_j(\lambda, \Omega_1) \quad (70)$$

$$\delta g_j(\lambda, \Omega_0, \Omega_1) = \Delta g_j(\lambda, \Omega_0) + g_j(\lambda, \Omega_1) = g_j(\lambda) + \Delta g_j(\lambda, \Omega_0) - \Delta g_j(\lambda, \Omega_1) \quad (71)$$

$$\delta h_j(\lambda, \Omega_0, \Omega_1) = \Delta h_j(\lambda, \Omega_0) + h_j(\lambda, \Omega_1) = h_j(\lambda) + \Delta h_j(\lambda, \Omega_0) - \Delta h_j(\lambda, \Omega_1) \quad (72)$$

Three Parameter Model of Undetrended Terrain Roughness Data

This section considers the use of undetrended nonstationary elevation profiles to determine the surface roughness power spectrum. If the terrain roughness power spectrum has $E < 0$ as in cases Type 3 and Type 4 of Figure 2b there is a lower cutoff frequency Ω_0 for the power spectrum and the difficulties associated with integrals for $\Omega \rightarrow 0$ do not arise. For this case undetrended roughness data can be used to determine the power spectrum coefficients C , D and E , and a detrending constant λ does not enter into the calculations. Types 1, 2 and 5 power spectra do not have a lower cutoff frequency and therefore must be obtained from detrended data.

Type 3 Power Spectrum

For a Type 3 roughness power spectrum that exhibits a lower frequency cut-off, the integrals expressing σ_d , σ_s and σ_c for undetrended data in terms of the power spectrum coefficients are (see Figure 2b)

$$\sigma_d^2 = \int_{\Omega_0}^{\infty} (C\Omega^{-2} + D\Omega^{-3} + E\Omega^{-4}) d\Omega = Cf_1(\Omega_0) + Df_2(\Omega_0) + Ef_3(\Omega_0) \quad (73)$$

$$\begin{aligned} \sigma_s^2 &= \left(\frac{2\pi}{a}\right)^2 \int_{\Omega_0}^{\infty} (C\Omega^{-2} + D\Omega^{-3} + E\Omega^{-4}) \sin^2(a\Omega) d\Omega \\ &= Cg_1(\Omega_0) + Dg_2(\Omega_0) + Eg_3(\Omega_0) \end{aligned} \quad (74)$$

$$\begin{aligned} \sigma_c^2 &= \left(\frac{2\pi}{a}\right)^4 \int_{\Omega_0}^{\infty} (C\Omega^{-2} + D\Omega^{-3} + E\Omega^{-4}) \sin^4(a\Omega) d\Omega \\ &= Ch_1(\Omega_0) + Dh_2(\Omega_0) + Eh_3(\Omega_0) \end{aligned} \quad (75)$$

where σ_d , σ_s and σ_c are obtained from undetrended data.

The integrals to be evaluated are

$$f_1(\Omega_0) = \int_{\Omega_0}^{\infty} \frac{d\Omega}{\Omega^2} \quad (76)$$

$$f_2(\Omega_0) = \int_{\Omega_0}^{\infty} \frac{d\Omega}{\Omega^3} \quad (77)$$

$$f_3(\Omega_0) = \int_{\Omega_0}^{\infty} \frac{d\Omega}{\Omega^4} \quad (78)$$

$$g_1(\Omega_0) = \left(\frac{2\pi}{a}\right)^2 \int_{\Omega_0}^{\infty} \frac{\sin^2(a\Omega) d\Omega}{\Omega^2} \quad (79)$$

$$g_2(\Omega_0) = \left(\frac{2\pi}{a}\right)^2 \int_{\Omega_0}^{\infty} \frac{\sin^2(a\Omega) d\Omega}{\Omega^3} \quad (80)$$

$$g_3(\Omega_0) = \left(\frac{2\pi}{a}\right)^2 \int_{\Omega_0}^{\infty} \frac{\sin^2(a\Omega) d\Omega}{\Omega^4} \quad (81)$$

$$h_1(\Omega_0) = \left(\frac{2\pi}{a}\right)^4 \int_{\Omega_0}^{\infty} \frac{\sin^4(a\Omega) d\Omega}{\Omega^2} \quad (82)$$

$$h_2(\Omega_0) = \left(\frac{2\pi}{a}\right)^4 \int_{\Omega_0}^{\infty} \frac{\sin^4(a\Omega) d\Omega}{\Omega^3} \quad (83)$$

$$h_3(\Omega_0) = \left(\frac{2\pi}{a}\right)^4 \int_{\Omega_0}^{\infty} \frac{\sin^4(a\Omega) d\Omega}{\Omega^4} \quad (84)$$

The integrals $f_1(\Omega_0)$, $f_2(\Omega_0)$, $f_3(\Omega_0)$, $g_2(\Omega_0)$, and $g_3(\Omega_0)$ diverge in the long wavelength limit $\Omega_0 \rightarrow 0$.

The evaluation of these integrals is done in Reference 1 and yields the following results

$$f_1(\Omega_0) \approx \Omega_0^{-1} \quad (85)$$

$$f_2(\Omega_0) = \frac{\Omega_0^{-2}}{2} \quad (86)$$

$$f_3(\Omega_0) = \frac{\Omega_0^{-3}}{3} \quad (87)$$

$$g_1(\Omega_0) = \frac{2\pi^2}{a^2} \left(\frac{1}{\Omega_0} - I_2^{(2a)} \right) \quad (88)$$

$$g_2(\Omega_0) = \frac{2\pi^2}{a^2} \left(\frac{1}{2\Omega_0^2} - I_3^{(2a)} \right) \quad (89)$$

$$g_3(\Omega_0) = \frac{2\pi^2}{a^2} \left(\frac{1}{3\Omega_0^3} - I_4^{(2a)} \right) \quad (90)$$

$$h_1(\Omega_0) = \left(\frac{2\pi}{a}\right)^4 \left(\frac{3}{8} \frac{1}{\Omega_0} - \frac{1}{2} I_2^{(2a)} + \frac{1}{8} I_2^{(4a)} \right) \quad (91)$$

$$h_2(\Omega_0) = \left(\frac{2\pi}{a}\right)^4 \left(\frac{3}{16} \frac{1}{\Omega_0^2} - \frac{1}{2} I_3^{(2a)} + \frac{1}{8} I_3^{(4a)} \right) \quad (92)$$

$$h_3(\Omega_0) = \left(\frac{2\pi}{a}\right)^4 \left(\frac{1}{8} \frac{1}{\Omega_0^3} - \frac{1}{2} I_4^{(2a)} + \frac{1}{8} I_4^{(4a)} \right) \quad (93)$$

where the I 's are given by

$$I_2^{(2a)} = \frac{\cos(2a\Omega_0)}{\Omega_0} + 2a \operatorname{si}(2a\Omega_0) \quad (94)$$

$$I_3^{(2a)} = \frac{\cos(2a\Omega_0)}{2\Omega_0^2} - \frac{a \sin(2a\Omega_0)}{\Omega_0} + 2a^2 \operatorname{Ci}(2a\Omega_0) \quad (95)$$

$$I_4^{(2a)} = \frac{\cos(2a\Omega_0)}{3\Omega_0^3} - \frac{2 \sin(2a\Omega_0)}{3\Omega_0^2} - \frac{2a^2 \cos(2a\Omega_0)}{3\Omega_0} - \frac{4}{3} a^3 \operatorname{si}(2a\Omega_0) \quad (96)$$

$$I_2^{(4a)} = \frac{\cos(4a\Omega_0)}{\Omega_0} + 4a \operatorname{si}(4a\Omega_0) \quad (97)$$

$$I_3^{(4a)} = \frac{\cos(4a\Omega_0)}{2\Omega_0^2} - \frac{2a \sin(4a\Omega_0)}{\Omega_0} + 8a^2 \operatorname{Ci}(4a\Omega_0) \quad (98)$$

$$I_4^{(4a)} = \frac{\cos(4a\Omega_0)}{3\Omega_0^3} - \frac{2a \sin(4a\Omega_0)}{3\Omega_0^2} - \frac{8a^2 \cos(4a\Omega_0)}{3\Omega_0} - \frac{32}{3} a^3 \operatorname{si}(4a\Omega_0) \quad (99)$$

and where sine integral and cosine integral functions are given by

$$\text{si}(t) = \int_{-\infty}^t \frac{\sin x}{x} dx = -\frac{\pi}{2} + t - \frac{t^3}{3!3} + \frac{t^5}{5!5} - \frac{t^7}{7!7} + \dots \quad (100)$$

$$\text{Ci}(t) = \int_{-\infty}^t \frac{\cos x}{x} dx = \gamma + \log_e t - \frac{t^2}{2!2} + \frac{t^4}{4!4} - \frac{t^6}{6!6} + \dots \quad (101)$$

where γ = Euler constant = 0.5772157. This completes the analytical evaluation of the integrals $f_j(\Omega_0)$, $g_j(\Omega_0)$ and $h_j(\Omega_0)$.

Type 4 Power Spectrum

A Type 4 roughness power spectrum exhibits a spectral window having lower and upper frequency cutoffs Ω_0 and Ω_1 respectively. The integrals defining σ_d , σ_s and σ_c are written as (see Figure 2b)

$$\sigma_d^2 = \int_{\Omega_0}^{\Omega_1} (C\Omega^{-2} + D\Omega^{-3} + E\Omega^{-4}) d\Omega = Cf_1(\Omega_0, \Omega_1) + Df_2(\Omega_0, \Omega_1) + Ef_3(\Omega_0, \Omega_1) \quad (102)$$

$$\begin{aligned} \sigma_s^2 &= \left(\frac{2\pi}{a}\right)^2 \int_{\Omega_0}^{\Omega_1} (C\Omega^{-2} + D\Omega^{-3} + E\Omega^{-4}) \sin^2(a\Omega) d\Omega \\ &= Cg_1(\Omega_0, \Omega_1) + Dg_2(\Omega_0, \Omega_1) + Eg_3(\Omega_0, \Omega_1) \end{aligned} \quad (103)$$

$$\begin{aligned} \sigma_c^2 &= \left(\frac{2\pi}{a}\right)^4 \int_{\Omega_0}^{\Omega_1} (C\Omega^{-2} + D\Omega^{-3} + E\Omega^{-4}) \sin^4(a\Omega) d\Omega \\ &= Ch_1(\Omega_0, \Omega_1) + Dh_2(\Omega_0, \Omega_1) + Eh_3(\Omega_0, \Omega_1) \end{aligned} \quad (104)$$

where σ_d , σ_s and σ_c refer to undetrended data, and where the integrals $f_j(\Omega_0, \Omega_1)$, $g_j(\Omega_0, \Omega_1)$, and $h_j(\Omega_0, \Omega_1)$ must be evaluated analytically.

By writing the integrals in equations (102), (103) and (104) as $\int_{\Omega_0}^{\Omega_1} = \int_{\Omega_0}^{\infty} - \int_{\Omega_1}^{\infty}$, the following values of these integrals are obtained.

$$f_j(\Omega_0, \Omega_1) = f_j(\Omega_0) - f_j(\Omega_1) \quad (105)$$

$$g_j(\Omega_0, \Omega_1) = g_j(\Omega_0) - g_j(\Omega_1) \quad (106)$$

$$h_j(\Omega_0, \Omega_1) = h_j(\Omega_0) - h_j(\Omega_1) \quad (107)$$

where the functions $f_j(\Omega)$, $g_j(\Omega)$, and $h_j(\Omega)$ are given by equations (85) through (93).

Calculations of the Parameters of the Roughness Power Spectrum

This section gives the procedure for explicitly calculating the power spectrum coefficients C, D and E, and also the cutoff frequencies Ω_0 and Ω_1 which occur in Type 1 - Type 5 power spectra. The values of the integrals $f_j(\lambda)$, $g_j(\lambda)$, $h_j(\lambda)$, and $\Delta f_j(\lambda, \Omega_0)$, $\Delta g_j(\lambda, \Omega_0)$, and $\Delta h_j(\lambda, \Omega_0)$ for the detrended case; $f_j(\Omega_0)$, $g_j(\Omega_0)$, and $h_j(\Omega_0)$ for the Type 3 undetrended case; and $f_j(\Omega_0, \Omega_1)$, $g_j(\Omega_0, \Omega_1)$, and $h_j(\Omega_0, \Omega_1)$ for the Type 4 undetrended case have now been evaluated. These integrals are used to calculate the coefficients C, D and E (and Ω_0 and Ω_1 where necessary) that describe the power spectrum of the actual terrain elevation profile.

The detrending procedure can be applied whether or not there is a lower cutoff frequency Ω_0 , and therefore this procedure can be applied to all of the five power spectrum types shown in Figure 2b. The detrending procedure must be applied to power spectra of Types 1, 2 and 5 because these cases have positive values of power spectrum in the limit $\Omega \rightarrow 0$. For Types 3 and 4 power spectra either the detrended or the undetrended formalism can be used. First the calculation of C, D and E for all five types of terrain roughness will be done using the detrended scheme, and then C, D and E will be calculated for spectral types 3 and 4 using the undetrended scheme.

Detrended Scheme

Type 1 ($C > 0$, $D > 0$, $E > 0$), Figure 2b.

The three simultaneous equations (17) - (19) yield

$$C = \frac{\begin{vmatrix} V_d & f_2(\lambda) & f_3(\lambda) \\ V_d & g_2(\lambda) & g_3(\lambda) \\ V_s & h_2(\lambda) & h_3(\lambda) \end{vmatrix}}{\text{DET}(\lambda)} \quad D = \frac{\begin{vmatrix} f_1(\lambda) & V_d & f_3(\lambda) \\ g_1(\lambda) & V_d & g_3(\lambda) \\ h_1(\lambda) & V_s & h_3(\lambda) \end{vmatrix}}{\text{DET}(\lambda)} \quad (108)$$

$$E = \frac{\begin{vmatrix} f_1(\lambda) & f_2(\lambda) & V_d \\ g_1(\lambda) & g_2(\lambda) & V_s \\ h_1(\lambda) & h_2(\lambda) & V_c \end{vmatrix}}{\text{DET}(\lambda)} \quad \text{DET}(\lambda) = \begin{vmatrix} f_1(\lambda) & f_2(\lambda) & f_3(\lambda) \\ g_1(\lambda) & g_2(\lambda) & g_3(\lambda) \\ h_1(\lambda) & h_2(\lambda) & h_3(\lambda) \end{vmatrix} \quad (109)$$

which give C, D and E in terms of the measured variances V_d , V_s and V_c of detrended data.

Type 2 ($C < 0$, $D \leq 0$, $E > 0$), Figure 2b.

The solution of the three simultaneous equations (17) - (19) give the power spectrum coefficients as

$$C = \frac{\begin{vmatrix} V_d & \Delta f_2(\lambda, \Omega_0) & \Delta f_3(\lambda, \Omega_0) \\ V_s & \Delta g_2(\lambda, \Omega_0) & \Delta g_3(\lambda, \Omega_0) \\ V_c & \Delta h_2(\lambda, \Omega_0) & \Delta h_3(\lambda, \Omega_0) \end{vmatrix}}{\text{DET}\Delta(\lambda, \Omega_0)} \quad D = \frac{\begin{vmatrix} \Delta f_1(\lambda, \Omega_0) & V_d & \Delta f_3(\lambda, \Omega_0) \\ \Delta g_1(\lambda, \Omega_0) & V_s & \Delta g_3(\lambda, \Omega_0) \\ \Delta h_1(\lambda, \Omega_0) & V_c & \Delta h_3(\lambda, \Omega_0) \end{vmatrix}}{\text{DET}\Delta(\lambda, \Omega_0)} \quad (110)$$

$$E = \frac{\begin{vmatrix} \Delta f_1(\lambda, \Omega_0) & \Delta f_2(\lambda, \Omega_0) & V_d \\ \Delta g_1(\lambda, \Omega_0) & \Delta g_2(\lambda, \Omega_0) & V_s \\ \Delta h_1(\lambda, \Omega_0) & \Delta h_2(\lambda, \Omega_0) & V_c \end{vmatrix}}{\text{DET}\Delta(\lambda, \Omega_0)} \quad \text{DET}\Delta(\lambda, \Omega_0) = \begin{vmatrix} \Delta f_1(\lambda, \Omega_0) & \Delta f_2(\lambda, \Omega_0) & \Delta f_3(\lambda, \Omega_0) \\ \Delta g_1(\lambda, \Omega_0) & \Delta g_2(\lambda, \Omega_0) & \Delta g_3(\lambda, \Omega_0) \\ \Delta h_1(\lambda, \Omega_0) & \Delta h_2(\lambda, \Omega_0) & \Delta h_3(\lambda, \Omega_0) \end{vmatrix} \quad (111)$$

and the equation for Ω_0 as

$$\Omega_0 = \frac{-D - \sqrt{D^2 - 4CE}}{2C} \quad (112)$$

These four equations determine C, D, E and Ω_0 .

Type 3 ($C > 0$, $D \geq 0$, $E < 0$), Figure 2b.

The solution of the three simultaneous equations (17) - (19) give the following expressions for the power spectrum coefficients

$$C = \frac{\begin{vmatrix} v_d & f_2(\lambda, \Omega_0) & f_3(\lambda, \Omega_0) \\ v_d & g_2(\lambda, \Omega_0) & g_3(\lambda, \Omega_0) \\ v_c^s & h_2(\lambda, \Omega_0) & h_3(\lambda, \Omega_0) \end{vmatrix}}{\text{DET}(\lambda, \Omega_0)} \quad D = \frac{\begin{vmatrix} f_1(\lambda, \Omega_0) & v_d & f_3(\lambda, \Omega_0) \\ g_1(\lambda, \Omega_0) & v_d & g_3(\lambda, \Omega_0) \\ h_1(\lambda, \Omega_0) & v_c^s & h_3(\lambda, \Omega_0) \end{vmatrix}}{\text{DET}(\lambda, \Omega_0)} \quad (113)$$

$$E = \frac{\begin{vmatrix} f_1(\lambda, \Omega_0) & f_2(\lambda, \Omega_0) & v_d \\ g_1(\lambda, \Omega_0) & g_2(\lambda, \Omega_0) & v_d^s \\ h_1(\lambda, \Omega_0) & h_2(\lambda, \Omega_0) & v_c^s \end{vmatrix}}{\text{DET}(\lambda, \Omega_0)} \quad \text{DET}(\lambda, \Omega_0) = \begin{vmatrix} f_1(\lambda, \Omega_0) & f_2(\lambda, \Omega_0) & f_3(\lambda, \Omega_0) \\ g_1(\lambda, \Omega_0) & g_2(\lambda, \Omega_0) & g_3(\lambda, \Omega_0) \\ h_1(\lambda, \Omega_0) & h_2(\lambda, \Omega_0) & h_3(\lambda, \Omega_0) \end{vmatrix} \quad (114)$$

and the following equation for Ω_0

$$\Omega_0 = \frac{-D + \sqrt{D^2 - 4CE}}{2C} \quad (115)$$

These four equations determine the four unknowns C, D, E and Ω_0 . The variances v_d , v_s and v_c refer to data detrended with the constant λ .

Type 4 ($C < 0$, $D > 0$, $E < 0$), Figure 2b.

The three simultaneous equations (17) - (19) yield

$$C = \frac{\begin{vmatrix} v_d & f_2(\lambda, \Omega_0, \Omega_1) & f_3(\lambda, \Omega_0, \Omega_1) \\ v_d & g_2(\lambda, \Omega_0, \Omega_1) & g_3(\lambda, \Omega_0, \Omega_1) \\ v_c^s & h_2(\lambda, \Omega_0, \Omega_1) & h_3(\lambda, \Omega_0, \Omega_1) \end{vmatrix}}{\text{DET}(\lambda, \Omega_0, \Omega_1)} \quad D = \frac{\begin{vmatrix} f_1(\lambda, \Omega_0, \Omega_1) & v_d & f_3(\lambda, \Omega_0, \Omega_1) \\ g_1(\lambda, \Omega_0, \Omega_1) & v_d & g_3(\lambda, \Omega_0, \Omega_1) \\ h_1(\lambda, \Omega_0, \Omega_1) & v_c^s & h_3(\lambda, \Omega_0, \Omega_1) \end{vmatrix}}{\text{DET}(\lambda, \Omega_0, \Omega_1)} \quad (116)$$

$$E = \frac{\begin{vmatrix} f_1(\lambda, \Omega_0, \Omega_1) & f_2(\lambda, \Omega_0, \Omega_1) & v_d \\ g_1(\lambda, \Omega_0, \Omega_1) & g_2(\lambda, \Omega_0, \Omega_1) & v_d^s \\ h_1(\lambda, \Omega_0, \Omega_1) & h_2(\lambda, \Omega_0, \Omega_1) & v_c^s \end{vmatrix}}{\text{DET}(\lambda, \Omega_0, \Omega_1)} \quad (117)$$

$$\text{DET}(\lambda, \Omega_0, \Omega_1) = \begin{vmatrix} f_1(\lambda, \Omega_0, \Omega_1) & f_2(\lambda, \Omega_0, \Omega_1) & f_3(\lambda, \Omega_0, \Omega_1) \\ g_1(\lambda, \Omega_0, \Omega_1) & g_2(\lambda, \Omega_0, \Omega_1) & g_3(\lambda, \Omega_0, \Omega_1) \\ h_1(\lambda, \Omega_0, \Omega_1) & h_2(\lambda, \Omega_0, \Omega_1) & h_3(\lambda, \Omega_0, \Omega_1) \end{vmatrix}$$

and the following equations for the bandwidth

$$\Omega_0 = \frac{-D + \sqrt{D^2 - 4CE}}{2C} \quad (118)$$

$$\Omega_1 = \frac{-D - \sqrt{D^2 - 4CE}}{2C} \quad (119)$$

These five equations determine the five unknown power spectrum parameters C, D, E, Ω_0 and Ω_1 .

Type 5B ($C > 0$, $D < 0$, $E > 0$), Figure 2b.

The three simultaneous equations (17) - (19) yield

$$C = \frac{\begin{vmatrix} V_d & \delta f_2(\lambda, \Omega_0, \Omega_1) & \delta f_3(\lambda, \Omega_0, \Omega_1) \\ V_c & \delta g_2(\lambda, \Omega_0, \Omega_1) & \delta g_3(\lambda, \Omega_0, \Omega_1) \\ V_c^s & \delta h_2(\lambda, \Omega_0, \Omega_1) & \delta h_3(\lambda, \Omega_0, \Omega_1) \end{vmatrix}}{\text{DET}(\lambda, \Omega_0, \Omega_1)} \quad D = \frac{\begin{vmatrix} \delta f_1(\lambda, \Omega_0, \Omega_1) & V_d & \delta f_3(\lambda, \Omega_0, \Omega_1) \\ \delta g_1(\lambda, \Omega_0, \Omega_1) & V_d & \delta g_3(\lambda, \Omega_0, \Omega_1) \\ \delta h_1(\lambda, \Omega_0, \Omega_1) & V_c^s & \delta h_3(\lambda, \Omega_0, \Omega_1) \end{vmatrix}}{\text{DET}(\lambda, \Omega_0, \Omega_1)} \quad (120)$$

$$E = \frac{\begin{vmatrix} \delta f_1(\lambda, \Omega_0, \Omega_1) & \delta f_2(\lambda, \Omega_0, \Omega_1) & V_d \\ \delta g_1(\lambda, \Omega_0, \Omega_1) & \delta g_2(\lambda, \Omega_0, \Omega_1) & V_d \\ \delta h_1(\lambda, \Omega_0, \Omega_1) & \delta h_2(\lambda, \Omega_0, \Omega_1) & V_c^s \end{vmatrix}}{\text{DET}(\lambda, \Omega_0, \Omega_1)} \quad (121)$$

$$\text{DET}(\lambda, \Omega_0, \Omega_1) = \begin{vmatrix} \delta f_1(\lambda, \Omega_0, \Omega_1) & \delta f_2(\lambda, \Omega_0, \Omega_1) & \delta f_3(\lambda, \Omega_0, \Omega_1) \\ \delta g_1(\lambda, \Omega_0, \Omega_1) & \delta g_2(\lambda, \Omega_0, \Omega_1) & \delta g_3(\lambda, \Omega_0, \Omega_1) \\ \delta h_1(\lambda, \Omega_0, \Omega_1) & \delta h_2(\lambda, \Omega_0, \Omega_1) & \delta h_3(\lambda, \Omega_0, \Omega_1) \end{vmatrix}$$

The equations for Ω_0 and Ω_1 are

$$\Omega_0 = \frac{-D - \sqrt{D^2 - 4CE}}{2C} \quad (122)$$

$$\Omega_1 = \frac{-D + \sqrt{D^2 - 4CE}}{2C} \quad (123)$$

These five equations determine C, D, E, Ω_0 and Ω_1 .

For the detrended scheme the values of σ_d , σ_s and σ_c are obtained from data measured at intervals of ΔL and detrended with a factor λ . As such σ_d , σ_s and σ_c represent data that have been conditioned in order that the theoretical determination of C, D and E can be accomplished by equations (17) - (19). The expressions for ϕ^{-2} and $\sin(a\Omega)/a\Omega$ that occur in the right hand sides of equations (17) - (19) account for the detrending factor λ and the measurement interval ΔL , so that in principle the coefficients C, D and E are independent of the intervals of data measurement or the detrending technique, and reflect the actual roughness condition of the terrain. It is clear then that, as written in equation (14) through (16), P_d describes actual surface roughness, while P_s and P_c still contain a factor containing the arbitrarily selected value of ΔL . But ΔL can be set to zero at this point of the calculation to obtain the values of P_s and P_c for the actual terrain.

This concludes the calculation procedure of the power spectrum coefficients C, D and E from detrended elevation profile data.

Undetrended Scheme

Only Type 3 and Type 4 power spectra can be handled using undetrended data.

Type 3 ($C > 0$, $D \geq 0$, $E < 0$), Figure 2b.

For a Type 1 power spectrum the undetrended elevation profile can be used, and the power spectrum coefficients are determined by

$$C = \frac{\begin{vmatrix} V & f_2(\Omega_0) & f_3(\Omega_0) \\ V_d & g_2(\Omega_0) & g_3(\Omega_0) \\ V_s & h_2(\Omega_0) & h_3(\Omega_0) \end{vmatrix}}{\text{DET}(\Omega_0)} \quad D = \frac{\begin{vmatrix} f_1(\Omega_0) & V & f_3(\Omega_0) \\ g_1(\Omega_0) & V_d & g_3(\Omega_0) \\ h_1(\Omega_0) & V_s & h_3(\Omega_0) \end{vmatrix}}{\text{DET}(\Omega_0)} \quad (124)$$

$$E = \frac{\begin{vmatrix} f_1(\Omega_0) & f_2(\Omega_0) & V_d \\ g_1(\Omega_0) & g_2(\Omega_0) & V_s \\ h_1(\Omega_0) & h_2(\Omega_0) & V_c \end{vmatrix}}{\text{DET}(\Omega_0)} \quad \text{DET}(\Omega_0) = \begin{vmatrix} f_1(\Omega_0) & f_2(\Omega_0) & f_3(\Omega_0) \\ g_1(\Omega_0) & g_2(\Omega_0) & g_3(\Omega_0) \\ h_1(\Omega_0) & h_2(\Omega_0) & h_3(\Omega_0) \end{vmatrix} \quad (125)$$

and the following equation for Ω_0

$$\Omega_0 = \frac{-D + \sqrt{D^2 - 4CE}}{2C} \quad (126)$$

These four equations determine the four unknowns C, D, E and Ω_0 that describe a Type 3 power spectrum. The variances V_d , V_s and V_c refer to undetrended elevation profile data.

Type 4 ($C < 0$, $D > 0$, $E < 0$), Figure 2b.

For an undetrended elevation profile with a Type 4 power spectrum of bandwidth $\Omega_1 - \Omega_0$, the power spectrum is calculated by

$$C = \frac{\begin{vmatrix} V_d & f_2(\Omega_0, \Omega_1) & f_3(\Omega_0, \Omega_1) \\ V_d & g_2(\Omega_0, \Omega_1) & g_3(\Omega_0, \Omega_1) \\ V_c^s & h_2(\Omega_0, \Omega_1) & h_3(\Omega_0, \Omega_1) \end{vmatrix}}{\text{DET}(\Omega_0, \Omega_1)} \quad D = \frac{\begin{vmatrix} f_1(\Omega_0, \Omega_1) & V_d & f_3(\Omega_0, \Omega_1) \\ g_1(\Omega_0, \Omega_1) & V_d & g_3(\Omega_0, \Omega_1) \\ h_1(\Omega_0, \Omega_1) & V_c^s & h_3(\Omega_0, \Omega_1) \end{vmatrix}}{\text{DET}(\Omega_0, \Omega_1)} \quad (127)$$

$$E = \frac{\begin{vmatrix} f_1(\Omega_0, \Omega_1) & f_2(\Omega_0, \Omega_1) & V_d \\ g_1(\Omega_0, \Omega_1) & g_2(\Omega_0, \Omega_1) & V_d \\ h_1(\Omega_0, \Omega_1) & h_2(\Omega_0, \Omega_1) & V_c^s \end{vmatrix}}{\text{DET}(\Omega_0, \Omega_1)} \quad (128)$$

$$\text{DET}(\Omega_0, \Omega_1) = \begin{vmatrix} f_1(\Omega_0, \Omega_1) & f_2(\Omega_0, \Omega_1) & f_3(\Omega_0, \Omega_1) \\ g_1(\Omega_0, \Omega_1) & g_2(\Omega_0, \Omega_1) & g_3(\Omega_0, \Omega_1) \\ h_1(\Omega_0, \Omega_1) & h_2(\Omega_0, \Omega_1) & h_3(\Omega_0, \Omega_1) \end{vmatrix}$$

and the following equations for the bandwidth

$$\Omega_0 = \frac{-D + \sqrt{D^2 - 4CE}}{2C} \quad (129)$$

$$\Omega_1 = \frac{-D - \sqrt{D^2 - 4CE}}{2C} \quad (130)$$

These five equations determine the five unknowns C , D , E , Ω_0 and Ω_1 that describe the Type 4 power spectrum. The variances V_d , V_s and V_c refer to an undetrended elevation profile.

Dominant Frequencies of a Terrain Elevation Profile

Roughness power spectrum Types 3, 4 and 5 have a dominant wavelength for the undetrended elevation profile that can be calculated from equation (12) to be

$$\frac{1}{\lambda_D} = \Omega_D = \frac{-3D \pm \sqrt{9D^2 - 32CE}}{4C} \quad (131)$$

For detrended elevation profile data all five spectral types will have a dominant frequency. An approximate expression that gives the dominant wavelength of detrended elevation data in terms of σ_d and σ_s is

$$\lambda_D = \frac{1}{\Omega_D} = 2\pi \frac{\sigma_d}{\sigma_s} . \quad (132)$$

This expression is affected by the detrending process.

Numerical Analysis of Terrain Elevation Data

A numerical study was done to determine the types of terrain roughness power spectra that are associated with actual terrain areas, and to determine their basic frequency content. Computer program RRFN (Reference 1) was developed to calculate values of σ_d , σ_s and σ_c from a measured elevation profile.

The computer program RRFN performs the following specific functions:

- a. It detrends the measured elevation profile for some choice of value of the detrending parameter.
- b. It calculates the standard deviations of displacement, slope and curvature for the detrended and undetrended elevation profile.

Computer program TERR (Reference 1) was developed to calculate the roughness power spectra from the values of σ_d , σ_s and σ_c that are supplied by computer program RRFN. The computer program TERR contains all the integrals and mathematical functions that appear in Part II. Computer program TERR performs the following specific functions:

- a. It calculates the power spectrum parameters C, D and E and cutoff frequencies Ω_0 and Ω_1 from detrended values of σ_d , σ_s and σ_c for spectral Types 1 through 5, and from undetrended values of σ_d , σ_s and σ_c for spectral Types 3 and 4.
- b. It calculates the frequency dependence of all five types of terrain roughness power spectra.

The elevation profiles of 100 terrain sites were examined, and values of σ_d , σ_s and σ_c were calculated using computer program RRFN with a detrending constant $\lambda = 10$ ft. These values of σ_d , σ_s and σ_c were used as input for computer program TERR to calculate the values of the power spectrum coefficients C, D and E and the associated cutoff frequencies Ω_0 and Ω_1 that describe the spectral characteristics of the actual terrain. The results appear in Table 2. The values of C, D and E that appear in this table were calculated using the detrended data formalism.

The results in Table 2 show that the signs of the coefficients C, D and E can be positive or negative and the terrain sites can be separated into the five spectral classes described earlier and shown in Figure 2b. The frequency of occurrence is shown in Figure 2d which indicates that spectral Types 3, 4 and 5 are the most common spectral types.

Figures in Reference 1 show typical elevation profiles that correspond to the five types of roughness power spectra. These figures tend to support the conclusions that can be drawn from Figure 2b, namely: that Types 1 and 2 tend to contain mainly long wavelengths (20-60 ft) of relatively large amplitude, Types 3 and 4 tend to have a roughly sinusoidal pattern of medium sized amplitudes with medium sized wavelengths (5-10 ft), while Type 5 contains a high frequency component (wavelength less than 5 ft) of relatively small amplitude.

The frequency of occurrence of spectral types shown in Figure 2d probably depends on the type of terrain selected for this study in the sense that all of the areas selected were test sites used for the operation of vehicles. Other types of terrain, such as may be encountered in macroroughness studies like the elevations measured across a valley, may produce a somewhat different occurrence frequency diagram. The lengths of the elevation profiles used for this study were generally 300 ft. The selection of different profile lengths may also change the frequency occurrence diagram.

It was shown that spectral Types 3 and 4 exhibit a lower cutoff frequency Ω_0 and it is therefore possible to calculate the values of the power spectrum coefficients C, D and E using undetrended elevation profile data. Table 3 gives values of C, D and E calculated for Type 3 power spectra by both the detrended and the undetrended formalisms. The values of C, D and E predicted by both methods are essentially equal, as they should be since they refer to the natural terrain roughness and their values should be independent of the method of calculation.

The relationship of the values of σ_s and σ_c with the values of σ_d appears to be different for each of the five classes of terrain roughness. The relationship is shown in Figures 3a and 3b where it is seen that there is some tendency for the data to fall into distinct groups. Type 5 has the highest values of σ_s/σ_d and σ_c/σ_d due to the high frequency component associated with this spectral type. Types 1 and 2 have the lowest values of these ratios because they contain dominant low frequency components.

Figures 3c through 3e give the dependence of the values of σ_d , σ_s and σ_c on the choice of detrending parameter λ . The values of σ_d decrease rapidly with λ^{-1} , while the values of σ_s and σ_c decrease more slowly. The relatively slow variation of σ_s and σ_c with λ^{-1} indicates that these two quantities are associated with the higher frequency components of the terrain profile, while σ_d is associated with the lower frequencies.

The values of the spectral coefficients C, D and E immediately give the roughness power spectra for the terrain displacement, slope and curvature as given by equations (14) - (16). The basic forms of $P_d(\Omega)$, $P_s(\Omega)$ and $P_c(\Omega)$ are shown in Figures 4a through 6e for spectral Types 1 through 5.

PART III: GEOMETRY AND KINEMATICS OF THE VEHICLE - GROUND CONTACT

Introductory Remarks

In the previous parts of this paper, terrain roughness was described in a manner independent of the geometrical characteristics of an operating vehicle. But the degree of roughness of a terrain area, as measured by the dynamic response of an operating vehicle, will depend on the geometry of the vehicle-ground contact areas. Therefore the terrain roughness description introduced earlier in this paper must be generalized to include the effects of the geometry of the ground contact area.

Two kinds of quantities can be distinguished in vehicle dynamics problems--input and output variables. By input variables are meant all quantities measured or defined at the soil-vehicle contact points. Output quantities are all quantities measured or defined at points on the vehicle. A theoretical prediction of the output dynamical response of a vehicle requires an understanding of interaction of the geometry of the vehicle with the geometry of the ground surface because this interaction will produce a terrain roughness power spectrum that includes the effects of the terrain-vehicle contact geometry. This terrain-vehicle power spectrum serves as the input for calculations of the dynamical response of a vehicle. This part of the paper calculates the input power spectra for realistic vehicle-ground contact geometries.

Input Power Spectra for Single Point Contact with the Ground

This section derives the power spectra associated with the vertical velocity and acceleration of a point which is constrained to move along a specified elevation profile with a constant horizontal speed. This is done by first calculating the standard deviations of the vertical velocity and acceleration of the point in terms of the standard deviations of the slope and curvature.

The standard deviations of the vertical velocity and vertical acceleration of a point that follows the contours of the surface displacement profile are calculated as follows

$$\sigma_v^2 = \frac{1}{N} \sum_{j=1}^N \left(\frac{\Delta d_j}{\Delta t} \right)^2 = \frac{1}{N} u^2 \sum_{j=1}^N \left(\frac{\Delta d_j}{\Delta L} \right)^2 = u^2 \sigma_s^2 \quad (133)$$

$$\sigma_a^2 = \frac{1}{N} \sum_{j=1}^N \left(\frac{\Delta^2 d_j}{\Delta t^2} \right)^2 = \frac{1}{N} u^4 \sum_{j=1}^N \left(\frac{\Delta^2 d_j}{\Delta L^2} \right)^2 = u^4 \sigma_c^2 \quad (134)$$

where σ_v = standard deviation of vertical velocity of wheel-soil point of contact

σ_a = standard deviation of vertical acceleration of wheel-soil point of contact

v = vertical velocity of wheel-soil point of contact

a = vertical acceleration of wheel-soil point of contact

u = horizontal velocity of vehicle = $\frac{\Delta L}{\Delta t}$

Equations (133) and (134) are valid for both detrended and undetrended data. However, they are valid only for small values of slope, i.e. for the case when the curvature is essentially equal to the second derivative.

Therefore the RMS values of the slope and curvature immediately determine the RMS values of vertical velocity and vertical acceleration experienced by a point travelling over an elevation profile at a constant horizontal speed. This is done by

$$\sigma_v = u\sigma_s \quad (135)$$

$$\sigma_a = u^2\sigma_c \quad (136)$$

If the point travelling along the surface elevation has an associated mass, the standard deviation of the power delivered to this mass is approximately given by

$$\sigma_p = m\sigma_a\sigma_v = mu^3\sigma_s\sigma_c \quad (137)$$

where σ_p = standard deviation of power
 m = mass of point

Although the values of σ_v and σ_a are of some interest, they cannot be used directly to calculate the corresponding RMS values of output velocity and acceleration. The calculation of these output quantities requires the input power spectra.

The power spectral density functions for input displacement, slope, curvature, vertical velocity, and vertical acceleration for a point contact will not be calculated. The PSD functions are expressed in terms of the spatial frequency Ω or the time frequency f that are related as follows

$$\Omega = \frac{f}{u} \quad (138)$$

where f = time frequency. The PSD functions are defined as follows

$$\sigma_d^2 = \int_0^\infty P_d(\Omega) \phi^{-2} d\Omega = \int_0^\infty P'_d(f) \phi^{-2} df \quad (139)$$

$$\sigma_s^2 = \int_0^\infty P_s(\Omega) \phi^{-2} d\Omega = \int_0^\infty P'_s(f) \phi^{-2} df \quad (140)$$

$$\sigma_c^2 = \int_0^\infty P_c(\Omega) \phi^{-2} d\Omega = \int_0^\infty P'_c(f) \phi^{-2} df \quad (141)$$

$$\sigma_v^2 = \int_0^\infty P_v(\Omega) \phi^{-2} d\Omega = \int_0^\infty P'_v(f) \phi^{-2} df \quad (142)$$

$$\sigma_a^2 = \int_0^\infty P_a(\Omega) \phi^{-2} d\Omega = \int_0^\infty P'_a(f) \phi^{-2} df \quad (143)$$

where P_v = power spectrum of input velocity and P_a = power spectrum of input acceleration. Equations (138) through (143) can be used to determine the power spectra in terms of the time frequency.

From (133), (134) and (138) through (143) it follows that

$$P_v(\Omega) = u^2 P_s(\Omega) \quad (144)$$

$$P_a(\Omega) = u^4 P_c(\Omega) \quad (145)$$

Using (138) it is clear that

$$P'_d(f) = u^{-1} P_d(\Omega) \quad (146)$$

$$P'_s(f) = u^{-1} P_s(\Omega) \quad (147)$$

$$P'_c(f) = u^{-1} P_c(\Omega) \quad (148)$$

$$P'_v(f) = u^{-1} P_v(\Omega) = u P_s(\Omega) = u^2 P'_s(f) \quad (149)$$

$$P'_a(f) = u^{-1} P_a(\Omega) = u^3 P_c(\Omega) = u^4 P'_c(f) \quad (150)$$

A summary of the one point power spectra is given as follows. Let

$$\psi(\Omega) = C\Omega^{-2} + D\Omega^{-3} + E\Omega^{-4} \quad (151)$$

$$\psi\left(\frac{f}{u}\right) = C\left(\frac{u}{f}\right)^2 + D\left(\frac{u}{f}\right)^3 + E\left(\frac{u}{f}\right)^4 \quad (152)$$

then

$$P_d(\Omega) = \psi(\Omega) \quad (153)$$

$$P'_d(f) = u^{-1} \psi\left(\frac{f}{u}\right) = u^{-1} P_d(\Omega) \quad (154)$$

$$P_s(\Omega) = (2\pi\Omega)^2 P_d(\Omega) \quad (155)$$

$$P'_s(f) = \left(\frac{2\pi f}{u}\right)^2 P'_d(f) \quad (156)$$

$$P_c(\Omega) = (2\pi\Omega)^4 P_d(\Omega) \quad (157)$$

$$P'_c(f) = \left(\frac{2\pi f}{u}\right)^4 P'_d(f) \quad (158)$$

$$P_v(\Omega) = (2\pi u\Omega)^2 P_d(\Omega) \quad (159)$$

$$P'_v(f) = (2\pi f)^2 P'_d(f) \quad (160)$$

$$P_a(\Omega) = (2\pi u\Omega)^4 P_d(\Omega) \quad (161)$$

$$P'_a(f) = (2\pi f)^4 P'_d(f) \quad (162)$$

Table 1 gives the units of the various power spectra.

Input Power Spectra for a Two Point Contact with the Ground

The power spectra for the case of two contact points with the ground can be obtained by using the spectral window functions given in equations (15) and (16). The various kinematic and terrain roughness power spectral are then given by^{2, 4}

$$P_d(\Omega) = \psi(\Omega) \quad (163)$$

$$P'_d(f) = u^{-1} \psi\left(\frac{f}{u}\right) = u^{-1} P_d(\Omega) \quad (164)$$

$$P_s(\Omega) = (2\pi\Omega)^2 \left[\frac{\sin(a\Omega)}{a\Omega} \right]^2 P_d(\Omega) \quad (165)$$

$$P'_s(f) = \left(\frac{2\pi f}{u} \right)^2 \left[\frac{\sin(af/u)}{af/u} \right]^2 P'_d(f) \quad (166)$$

$$P_c(\Omega) = (2\pi\Omega)^4 \left[\frac{\sin(a\Omega)}{a\Omega} \right]^4 P_d(\Omega) \quad (167)$$

$$P'_c(f) = \left(\frac{2\pi f}{u} \right)^4 \left[\frac{\sin(af/u)}{af/u} \right]^4 P'_d(f) \quad (168)$$

$$P_v(\Omega) = (2\pi u\Omega)^2 \left[\frac{\sin(a\Omega)}{a\Omega} \right]^2 P_d(\Omega) \quad (169)$$

$$P'_v(f) = (2\pi f)^2 \left[\frac{\sin(af/u)}{af/u} \right]^2 P'_d(f) \quad (170)$$

$$P_a(\Omega) = (2\pi u\Omega)^4 \left[\frac{\sin(a\Omega)}{a\Omega} \right]^4 P_d(\Omega) \quad (171)$$

$$P'_a(f) = (2\pi f)^4 \left[\frac{\sin(af/u)}{af/u} \right]^4 P'_d(f) \quad (172)$$

where $a = \pi L$ and L = distance between the two contact points. The one point power spectra given in equations (153) through (162) are regained by taking $a = 0$ in equations (163) through (172), i.e., the spectral window functions have a unit value for the case of one point of contact.

Spectral Window Functions for Vehicles

The calculations of the input power spectra for vehicles requires a knowledge of the spectral window functions for vehicles. The slope and curvature spectral window functions were introduced in the roughness power spectrum calculations to account for the finite interval of measurement of the elevation profile. The same situation arises for a vehicle operating on a terrain site. When the absorbed power or vertical acceleration is measured at the driver's seat, the surface roughness is indirectly being measured. But now the sampling of the elevation profile is being done by the wheels of a truck or the track of a tank, and two physical situations must be considered. First, the sampling is done with finite contact lengths and second, there may be several unequal intervals of measurement as in the case of various distances between the wheels on one side of a truck running over an elevation profile. Both of these physical situations must be described to calculate the spectral window functions for vehicles.

The spectral window functions can be obtained by averaging over all possible two-point intervals along the areas of contact with the ground. The two-point contact spectral window functions for the slope and curvature are given by equations (15) and (16). Single and multiple contact areas must be considered for the averaging process using equations (15) and (16).

Single Contact Area

For the case of a single contact area, such as produced by one wheel or by a tank track, the spectral window functions are calculated by integrating equations (15) and (16) over all two-point contact positions as shown in Figure 7a with the result that

$$asw^{(2)} = \frac{1}{T_L^2} \int_0^{T_L} \int_0^{T_L} \frac{\sin^2 [\pi\Omega(x - y)]}{[\pi\Omega(x - y)]^2} dx dy \quad (173)$$

$$asw^{(4)} = \frac{1}{T_L^2} \int_0^{T_L} \int_0^{T_L} \frac{\sin^4 [\pi\Omega(x - y)]}{[\pi\Omega(x - y)]^4} dx dy \quad (174)$$

where

$asw^{(2)}$ = slope spectral window function for single contact area

$asw^{(4)}$ = curvature spectral window function for single contact area

T_L = length of contact area in the direction of vehicle motion

These spectral window functions are evaluated in Reference 1 and have the following values for small values of ΩT_L

$$\text{asw}^{(2)}(T_L) = 1 + \alpha_2(\Omega T_L)^2 + \alpha_4(\Omega T_L)^4 + \alpha_6(\Omega T_L)^6 + \dots \quad (175)$$

$$\text{asw}^{(4)}(T_L) = 1 + \beta_2(\Omega T_L)^2 + \beta_4(\Omega T_L)^4 + \beta_6(\Omega T_L)^6 + \dots \quad (176)$$

where

$$\alpha_2 = -\frac{\pi^2}{18} \quad (177)$$

$$\alpha_4 = +\frac{2\pi^4}{675} \quad (178)$$

$$\alpha_6 = -\frac{\pi^6}{8820} \quad (179)$$

$$\beta_2 = -\frac{\pi^2}{9} \quad (180)$$

$$\beta_4 = +\frac{\pi^4}{75} \quad (181)$$

$$\beta_6 = -\frac{17\pi^6}{13230} \quad (182)$$

These expressions are valid for $\Omega < 1/T_L$, and are therefore low frequency approximations.

For large values of ΩT_L (high frequency) these spectral window functions have the following asymptotic values

$$\text{asw}^{(2)} \sim \frac{1}{\Omega T_L} \quad (183)$$

$$\text{asw}^{(4)} \sim \frac{2}{3\Omega T_L} \quad (184)$$

The spectral window functions for the case of a single contact area are shown in Figure 7b.

Multiple Contact Areas

The calculation of the spectral window functions for a multiple contact area geometry, such as is produced by the wheels of a truck, is accomplished by integrating equations (15) and (16) over all two-point contact positions as shown in Figure 7c, with the result that

$$\begin{aligned} ASW^{(2)} = \frac{1}{(N + N!/2)T_L^2} & \left\{ \sum_{i=1}^N \int_0^{T_L} \int_0^{T_L} \frac{\sin^2 [\pi\Omega(\xi_i - \eta_i)]}{[\pi\Omega(\xi_i - \eta_i)]^2} d\xi_i d\eta_i \right. \\ & \left. + \sum_{\substack{i,j \\ i \neq j}}^N \int_{L_i}^{L_i+T_L} \int_{L_j}^{L_j+T_L} \frac{\sin^2 [\pi\Omega(\xi_i - \eta_j)]}{[\pi\Omega(\xi_i - \eta_j)]^2} d\xi_i d\eta_j \right\} \end{aligned} \quad (185)$$

$$\begin{aligned} ASW^{(4)} = \frac{1}{(N + N!/2)T_L^2} & \left\{ \sum_{i=1}^N \int_0^{T_L} \int_0^{T_L} \frac{\sin^4 [\pi\Omega(\xi_i - \eta_i)]}{[\pi\Omega(\xi_i - \eta_i)]^4} d\xi_i d\eta_i \right. \\ & \left. + \sum_{\substack{i,j \\ i \neq j}}^N \int_{L_i}^{L_i+T_L} \int_{L_j}^{L_j+T_L} \frac{\sin^4 [\pi\Omega(\xi_i - \eta_j)]}{[\pi\Omega(\xi_i - \eta_j)]^4} d\xi_i d\eta_j \right\} \end{aligned} \quad (186)$$

where

$ASW^{(2)}$ = slope spectral window function for a truck

$ASW^{(4)}$ = curvature spectral window function for a truck

N = number of wheels on one side of a truck

L_i = position of wheel i

L_j = position of wheel j

ξ_i, η_j = integration variables

In equations (185) and (186) it is assumed that all wheels of the truck are the same size. The truck spectral window functions are normalized by the factor $(N + N!/2)T_L^2$ to give a unit value if the truck dimensions were shrunk to zero size to produce the case of a one point contact.

The truck spectral window functions defined by equations (185) and (186) are evaluated in Reference 1 for the three types of wheel geometries shown in

Figure 7d. For this evaluation it is assumed that the wheel-ground contact length is equal to the tire radius, $T_L = T_R$ where T_R = tire radius.

a. Four wheel truck

$$ASW(2) = \frac{1}{3} \left\{ 2asw(2)(T_R) + \left[\frac{\sin(\pi L_{12}\Omega)}{\pi L_{12}\Omega} \right]^2 \right\} \quad (187)$$

$$ASW(4) = \frac{1}{3} \left\{ 2asw(4)(T_R) + \left[\frac{\sin(\pi L_{12}\Omega)}{\pi L_{12}\Omega} \right]^4 \right\} \quad (188)$$

b. Six wheel truck

$$ASW(2) = \frac{1}{6} \left\{ 3 asw(2)(T_R) + \left[\frac{\sin(\pi L_{12}\Omega)}{\pi L_{12}\Omega} \right]^2 + \left[\frac{\sin(\pi L_{13}\Omega)}{\pi L_{13}\Omega} \right]^2 + \left[\frac{\sin(\pi L_{23}\Omega)}{\pi L_{23}\Omega} \right]^2 \right\} \quad (189)$$

$$ASW(4) = \frac{1}{6} \left\{ 3 asw(4)(T_R) + \left[\frac{\sin(\pi L_{12}\Omega)}{\pi L_{12}\Omega} \right]^4 + \left[\frac{\sin(\pi L_{13}\Omega)}{\pi L_{13}\Omega} \right]^4 + \left[\frac{\sin(\pi L_{23}\Omega)}{\pi L_{23}\Omega} \right]^4 \right\} \quad (190)$$

c. Eight wheel truck

$$ASW(2) = \frac{1}{10} \left\{ 4 asw(2)(T_R) + \left[\frac{\sin(\pi L_{12}\Omega)}{\pi L_{12}\Omega} \right]^2 + \left[\frac{\sin(\pi L_{13}\Omega)}{\pi L_{13}\Omega} \right]^2 + \left[\frac{\sin(\pi L_{14}\Omega)}{\pi L_{14}\Omega} \right]^2 + \left[\frac{\sin(\pi L_{23}\Omega)}{\pi L_{23}\Omega} \right]^2 + \left[\frac{\sin(\pi L_{24}\Omega)}{\pi L_{24}\Omega} \right]^2 + \left[\frac{\sin(\pi L_{34}\Omega)}{\pi L_{34}\Omega} \right]^2 \right\} \quad (191)$$

$$ASW^{(4)} = \frac{1}{10} \left\{ 4 asw^{(4)}(T_R) + \left[\frac{\sin(\pi L_{12}\Omega)}{\pi L_{12}\Omega} \right]^4 + \left[\frac{\sin(\pi L_{13}\Omega)}{\pi L_{13}\Omega} \right]^4 + \left[\frac{\sin(\pi L_{14}\Omega)}{\pi L_{14}\Omega} \right]^4 + \left[\frac{\sin(\pi L_{23}\Omega)}{\pi L_{23}\Omega} \right]^4 + \left[\frac{\sin(\pi L_{24}\Omega)}{\pi L_{24}\Omega} \right]^4 + \left[\frac{\sin(\pi L_{34}\Omega)}{\pi L_{34}\Omega} \right]^4 \right\} \quad (192)$$

where L_{ij} = distance between wheels i and j . Figure 7e shows typical averaged slope and curvature spectral window functions for a four wheel truck.

Equations (187) through (192) show that the truck spectral window functions introduce the relevant geometrical characteristics of the wheel-ground contact, including wheel spacing and tire radius. Equations (175) through (184) show that the relevant geometrical quantity for track-laying vehicles is the track length in contact with the ground. All these equations can be easily generalized to the case of half-track vehicles.

Contact Length Filter

A vehicle will not respond to the high frequency components of a terrain elevation profile because the finite contact length of a tire or a track with the ground tends to filter out these frequencies. For instance a track of length T_L will filter out all wavelengths shorter than $T_L/2$, while on a smaller scale a tire of radius T_R will filter out wavelengths shorter than $T_R/2$. The situation is shown in Figure 8a.

A low pass filtering action due to the finite contact length with the ground is physically plausible and necessary, but a rigorous theoretical derivation of the form of this filter has not been developed. In this report it is assumed that the filter is of the exponential type

$$e^{-F(\Omega, T_L)} \quad (193)$$

where several forms of the filter function $F(\Omega, T_L)$ can be selected.

Two forms of the function $F(\Omega, T_L)$ were investigated in this report

$$F(\Omega, T_L) = \alpha \frac{\sigma_c}{\sigma_s} \Omega T_L = \alpha \frac{\sigma_c}{\sigma_s} \frac{T_L}{\lambda_w} \quad (194)$$

$$F(\Omega, T_L) = \beta (\Omega T_L)^2 = \beta \left(\frac{T_L}{\lambda_w} \right)^2 \quad (195)$$

where $\lambda_w = \Omega^{-1}$ = spatial wavelength. For the form appearing in equation (194) which is linear in T_L , it was found that a spatial frequency factor σ_c/σ_s had to be inserted to account for the dominant frequencies of the terrain. Only in this way was the parameter α found to have a constant value independent of terrain site and track length.

The values of α and β were determined empirically from experimental absorbed power data for trucks and track laying vehicles (see Part V) and are equal $\alpha = 118.8$ in. (for detrended values of σ_s and σ_c), $\alpha = 123.2$ in. for undetrended values of σ_s and σ_c) and $\beta = 1.4$.^s The form of the filter function given by equation (194) appears to describe the absorbed power data somewhat better than does the form in equation (195), so that all further calculations in this report were done using the filter function represented by equation (194). Figure 8b shows a typical exponential filter expressed in terms of ΩT_L .

The filter functions can also be written in terms of the time frequency using equation (138) as

$$F(f) = \alpha \frac{\sigma_c}{\sigma_s} \frac{f T_L}{u} = \alpha \frac{\sigma_c}{\sigma_s} f \tau \quad (196)$$

$$F(f) = \beta \left(\frac{f T_L}{u} \right)^2 = \beta (f \tau)^2 \quad (197)$$

where $\tau = T_L/u$ = time delay for transit of the vehicle-ground contact length.

Figure 8c shows a typical exponential filter, given by equation (196), expressed in terms of the time frequency.

INPUT POWER SPECTRA FOR VEHICLES. Taking the spectral window functions and the low pass contact length filter in account and treating vehicles as rigid bodies gives the following expressions for the input roughness power spectra and the input kinematic power spectra for wheeled vehicles:

$$P_{di}(\Omega) = e^{-F} P_d(\Omega) \quad (198)$$

$$P_{si}(\Omega) = (2\pi\Omega)^2 e^{-F} ASW^{(2)} P_d(\Omega) \quad (199)$$

$$P_{ci}(\Omega) = (2\pi\Omega)^4 e^{-F} ASW^{(4)} P_d(\Omega) \quad (200)$$

$$P_{vi}(\Omega) = (2\pi u\Omega)^2 e^{-F} ASW^{(2)} P_d(\Omega) \quad (201)$$

$$P_{ai}(\Omega) = (2\pi u \Omega)^4 e^{-F ASW^{(4)}} P_d(\Omega) \quad (202)$$

where P_{di} , P_{si} , P_{ci} , P_{vi} and P_{ai} = input vehicle power spectra for displacement, slope, curvature, vertical velocity and vertical acceleration respectively. These equations are valid for track vehicles with $ASW^{(2)}$ and $ASW^{(4)}$ replaced by $asw^{(2)}$ and $asw^{(4)}$ respectively.

Equations (198) through (202) show that the input kinematic power spectra for vehicles are related to the terrain roughness power spectrum that has been adjusted for vehicle geometry. The input kinematic power spectra would describe the motion of a vehicle if it were totally rigid. The actual vehicle response is calculated as a joint effect of these input kinematic power spectra and a transmission function which accounts for the impedance of the vehicle. The following Part IV develops the transmission function.

PART IV: DYNAMIC MODELS FOR MOVING VEHICLES

Introductory Remarks

It is of value to vehicle design engineers to be able to predict the vertical dynamic displacement, velocity and acceleration at a point on a moving vehicle and ultimately to predict the power absorbed by the driver. To do this, the dynamic response of a vehicle to rough terrain must be known. The dynamic response of a vehicle can be described by a transmission function.¹⁴⁻¹⁶

Because vehicles undergo pitching and rolling motions as well as vertical motion (heave), the power absorbed by the driver will depend critically on his location relative to the center of mass of the vehicle. It is important to be able to separate and determine the contributions to the absorbed power due to the surface roughness, the internal dynamics of the vehicle, and the location of the driver. The driver location variable appears in the pitching motion transmission function.

This paper uses simple linear viscoelastic spring models to describe the dynamic response of a vehicle. It is known that linear viscoelastic models do not adequately describe the dynamic properties of vehicles because the vehicles contain nonlinear springs and dashpots, and Coulomb damping in addition to viscoelastic damping. The linear viscoelastic models introduced here serve as a simple expedient way to evaluate the roughness power spectrum method.

The transmission functions developed will be used in Part V to calculate the power absorbed by the driver using a power spectrum method. The absorbed power calculation requires the output acceleration power spectrum at the drivers seat, and this can be calculated using a transmission function.

Vertical Motion Transmission Functions

Single Mass

Vertical Motion

The output power spectrum of a mechanical or structural system is related to the input power spectrum through the transmission function for the system, Figure 8d. The transmission function of a dynamical system is generally a complex number whose imaginary part is a measure of the damping. For a linear system the output power spectrum is given by

$$P_o'(f) = |T|^2 P_i'(f) \quad (203)$$

where $P_o'(f)$ = output power spectrum

T = transmission function

$|T|$ = magnitude of transmission function

$P'_i(f)$ = input power spectrum

Mechanical transmission functions generally come in two forms, one relating output displacement to input force, and the other relating output displacement to input displacement.

If the input to a linear spring system is a force and the output is a displacement we have

$$P'_{do} = |T_{dF}|^2 P'_{Fi} \quad (204)$$

where P'_{do} = power spectrum of the output displacement

T_{dF} = transmission function relating input dynamic force to the output dynamic displacement

P'_{Fi} = power spectrum of the input force

The transmission function for this case is⁴

$$T_{dF} = \frac{1/k}{1 - (f/f_n)^2 + i2\xi f/f_n} = |T_{dF}| e^{-i\phi_{dF}} \quad (205)$$

$$|T_{dF}|^2 = \frac{k^{-2}}{[1 - (f/f_n)^2]^2 + [2\xi f/f_n]^2} \quad (206)$$

$$\phi_{dF} = \tan^{-1} \left[\frac{2\xi f/f_n}{1 - (f/f_n)^2} \right] \quad (207)$$

where k = spring constant

$f_n = \sqrt{k/m}/2\pi$ = natural frequency

$\xi = C_D/(2\sqrt{km})$ = damping ratio

m = effective mass

C_D = damping constant

f = frequency

For application to vehicle dynamics a more useful transmission function is that which relates output displacement to input displacement. The output power spectrum of displacement is then given by

$$P'_{do}(f) = |T_{dd}|^2 P'_{di}(f) \quad (208)$$

where T_{dd} = transmission function relating the input dynamic displacement to the output dynamic displacement

P_{di} = power spectrum of input displacement

The transmission function for this case is given by⁴

$$T_{dd} = \frac{1 + i\sigma f}{1 - (f/f_n)^2 + i\sigma f} = |T_{dd}| e^{-i\phi_{dd}} \quad (209)$$

$$|T_{dd}|^2 = \frac{1 + \sigma^2 f^2}{[1 - (f/f_n)^2]^2 + \sigma^2 f^2} \quad (210)$$

$$\phi_{dd} = \tan^{-1} \left[\frac{\sigma f^3 / f_n^2}{1 - (f/f_n)^2 + \sigma^2 f^2} \right] \quad (211)$$

where $\sigma = 2\xi/f_n$. It is easy to show that the velocity-velocity transmission function and the acceleration-acceleration transmission function satisfy the following conditions

$$|T_{dd}| = |T_{vv}| = |T_{aa}| \quad (212)$$

where T_{vv} = transmission function relating input velocity to output velocity

T_{aa} = transmission function relating input acceleration to output acceleration

Therefore only the displacement-displacement transmission function needs to be considered for vehicle dynamics problems.

An important property of the transmission function is its value for zero frequency

$$T_{dd}(f = 0) = 1 \quad (213)$$

This corresponds to a simple translation of whole dynamic system, so that the static output displacement equals the static input displacement. Note also that $|T_{dd}|^2 \propto f^{-2}$ while $|T_{df}|^2 \propto f^{-4}$ in the high frequency limit. The transmission function for a vehicle running over rough terrain will depend on the vehicle speed because of the relation $f = u\Omega$. In particular, the value of $|T_{dd}|^2$ for the single degree of freedom model is obtained from equation (210) to be

$$|T_{dd}|^2 = \frac{1 + \sigma^2 u^2 \Omega^2}{(1 - u^2 \Omega^2 / f_n^2)^2 + \sigma^2 u^2 \Omega^2} \quad (214)$$

Note that for $u = 0$ the transmission function has the value of $|T_{dd}| = 1$.

Double Mass Vertical Motion

Vehicles generally exhibit two resonance peaks - one associated with the vertical motion of the body (~ 1 Hz) and the other with the vertical motion of the wheel suspension system (~ 15 Hz). A displacement-displacement transmission function for a two-mass system is therefore required to accurately describe the dynamic response of a vehicle moving over rough terrain. The derivation of the two-mass transmission function is given in Reference 1, and is as follows (Figure 9a)

$$T_{dd} = \frac{A + iB}{E + iF} \quad (215)$$

$$|T_{dd}|^2 = \frac{(AE + BF)^2 + (BE - AF)^2}{(E^2 + F^2)^2} \quad (216)$$

where

$$A = 1 - \frac{\omega^2 C_B C_W}{k_B k_W} \quad (217)$$

$$B = \omega \left(\frac{C_B}{k_B} + \frac{C_W}{k_W} \right) \quad (218)$$

$$E = \left(1 - \frac{\omega^2 M_W}{k_W} \right) \left(1 - \frac{\omega^2 M_B}{k_B} \right) - \omega^2 \left(\frac{C_B C_W}{k_B k_W} + \frac{M_B}{k_W} \right) \quad (219)$$

$$F = \omega \left\{ \frac{C_W}{k_W} + \frac{C_B}{k_B} - \omega^2 \left[\frac{M_B (C_B + C_W)}{k_B k_W} + \frac{M_W C_B}{k_B k_W} \right] \right\} \quad (220)$$

where $\omega = 2\pi f$

C_B = damping constant for vehicle body

C_W = damping constant for wheel suspension system

M_B = mass of vehicle body $= W_B/g$

M_W = mass of wheels $= W_W/g$

k_B = spring constant of vehicle body

k_W = spring constant of wheel suspension system

It appears that track laying vehicles can be adequately described by a single mass transmission function, while wheeled vehicles generally require a double mass transmission function to describe their vertical motion. Typical vertical motion transmission functions for tanks and trucks are shown in Figure 9b. The dynamical parameters for several track laying vehicles are given in Table 4, and for several trucks in Tables 5 and 6.

Combined Pitching and Vertical Motion Transmission Function

Because a vehicle operating on rough terrain has a pitching motion, the values of the power absorbed by the driver are expected to depend on the geometrical location of the driver relative to the center mass. The pitching motion of a vehicle can be described by a transmission function. This section calculates the displacement-displacement transmission function for a combined pitching and vertical mode of motion. The model used for this calculation is shown in Figure 9c, and consists of a rigid rod representing the vehicle body that is supported by two damped springs at each end.

The equations of motion for this model are the following coupled linear differential equations¹⁴

$$m\ddot{x} + k_1x_1 + C_1\dot{x}_1 + k_2x_2 + C_2\dot{x}_2 = k_1\eta_1 + C_1\dot{\eta}_1 + k_2\eta_2 + C_2\dot{\eta}_2 \quad (221)$$

$$J\ddot{\theta} - L_1[k_1x_1 + C_1\dot{x}_1] + L_2[k_2x_2 + C_2\dot{x}_2] = -L_1[k_1\eta_1 + C_1\dot{\eta}_1] + L_2[k_2\eta_2 + C_2\dot{\eta}_2] \quad (222)$$

where

m = mass of vehicle

\ddot{x} = vertical acceleration of center of mass

k_1 = equivalent spring constant of front support of vehicle

x_1 = vertical displacement of front support of vehicle

C_1 = equivalent damping of front support of vehicle

\dot{x}_1 = vertical velocity of front support of vehicle

k_2 = equivalent spring constant of rear support of vehicle

x_2 = vertical displacement of vehicle body directly above rear wheels

C_2 = equivalent damping constant of rear wheels and suspension
 \dot{x}_2 = vertical velocity of truck body directly above rear wheels
 η_1 = elevation of ground surface at front wheels
 $\dot{\eta}_1$ = rate of change of η_1 due to passing vehicle
 η_2 = elevation of ground surface at rear wheels
 $\dot{\eta}_2$ = time rate of change of η_2 due to moving vehicle
 J = moment of inertia about pitch axis through center of mass
 L_1 = distance from front of vehicle to center of mass
 L_2 = distance from rear of vehicle to center of mass

The solution of the coupled differential equations is given in Reference 1, and is given in the form of a transmission function. The displacement-displacement transmission function is given for a point in front of the center of mass and for a point behind the center of mass as follows

$$|T_F|^2 = (\xi_1^F)^2 + (\xi_2^F)^2 \quad (223)$$

$$|T_B|^2 = (\xi_1^B)^2 + (\xi_2^B)^2 \quad (224)$$

where

T_F = displacement-displacement transmission function for a point a distance z in front of the center of mass

T_B = displacement-displacement transmission function for a point a distance z behind the vehicle center of mass

z = distance from center of mass at which the motion is to be calculated

and where

$$\xi_1^F = R - zS \quad (225)$$

$$\xi_2^F = T - zU \quad (226)$$

$$\xi_1^B = R + zS \quad (227)$$

$$\xi_2^B = T + zU \quad (228)$$

$$R = (Z_1 W_1 + Z_2 W_2) / (W_1^2 + W_2^2) \quad (229)$$

$$S = (X_1 U_1 + X_2 U_2) / (U_1^2 + U_2^2) \quad (230)$$

$$T = (Z_2 W_1 - Z_1 W_2) / (W_1^2 + W_2^2) \quad (231)$$

$$U = (X_2 U_1 - U_2 X_1) / (U_1^2 + U_2^2) \quad (232)$$

$$Z_1 = \alpha_A (d - J\omega^2) - \omega\alpha_B g - b\beta_A + \omega h\beta_B \quad (233)$$

$$Z_2 = \alpha_B (d - J\omega^2) + \omega\alpha_A g - b\beta_B - \omega h\beta_A \quad (234)$$

$$W_1 = (k - m\omega^2)(d - J\omega^2) - \omega^2 Cg - b^2 + \omega^2 h^2 \quad (235)$$

$$W_2 = \omega C(d - J\omega^2) + \omega g(k - m\omega^2) - 2\omega b h \quad (236)$$

$$X_1 = \beta_A W_1 - \beta_B W_2 - bZ_1 + \omega hZ_2 \quad (237)$$

$$X_2 = \beta_B W_1 + \beta_A W_2 - bZ_2 - \omega hZ_1 \quad (238)$$

$$U_1 = W_1 (d - J\omega^2) - \omega g W_2 \quad (239)$$

$$U_2 = \omega g W_1 + W_2 (d - J\omega^2) \quad (240)$$

$$\alpha_A = k_1 + k_2 \cos (\omega L / u) + \omega C_2 \sin (\omega L / u) \quad (241)$$

$$\alpha_B = \omega C_1 - k_2 \sin (\omega L / u) + \omega C_2 \cos (\omega L / u) \quad (242)$$

$$\beta_A = L_2[k_2 \cos (\omega L/u) + \omega C_2 \sin (\omega L/u)] - L_1 k_1 \quad (243)$$

$$\beta_B = L_2[\omega C_2 \cos (\omega L/u) - k_2 \sin (\omega L/u)] - \omega C_1 L_1 \quad (244)$$

$$L = L_1 + L_2 \quad (245)$$

$$b = k_2 L_2 - k_1 L_1 \quad (246)$$

$$d = k_1 L_1^2 + k_2 L_2^2 \quad (247)$$

$$h = C_2 L_2 - C_1 L_1 \quad (248)$$

$$g = C_1 L_1^2 + C_2 L_2^2 \quad (249)$$

$$C = C_1 + C_2 \quad (250)$$

$$k = k_1 + k_2 \quad (251)$$

The derived transmission function can be used to calculate the motion of a vehicle at any position along the length of the vehicle relative to the center of mass. In this way a prediction of the dependence of the power absorbed by a driver on his location relative to the center of mass can be made. Figure 9d shows a typical transmission function for the combined vertical and pitching modes of motion.

PART V: ABSORBED POWER AND VEHICLE RESPONSE

Introductory Remarks

Quantities often measured for a vehicle moving over rough terrain are the power absorbed by the driver and the vertical acceleration at the drivers seat. The power absorbed by the driver is the energy dissipated as heat. It represents the energy lost due to vibration damping in the human body. Absorbed power is a physiological concept that has been developed as a measure of driver fatigue on prolonged exposure to vehicle induced vibrations.⁷ It has been found empirically that the maximum power that a driver can absorb and still function reasonably is six watts. Therefore it is of importance to be able to estimate the vehicle speed at which six watts of power is being dissipated by the driver. The six watt speed clearly depends on internal vehicle characteristics, the location of the driver relative to the center of mass of the vehicle, and the surface roughness.

Two methods are used to obtain the six watt speed. The first is a formal power spectrum method of calculating the power absorbed by the driver which includes a consideration of vehicle dynamics. The second is a regression analysis of the six watt speed measured for vehicles operating different types of terrain. The power spectrum method introduces the terrain roughness and vehicle geometry through the power spectra described in Parts II and III, and the vehicle dynamics through the transmission functions introduced in Part IV. The regression analysis uses directly the detrended values of σ_d , σ_s and σ_c to describe the terrain roughness, the track length or tire radius to describe the vehicle geometry, and the dimensionless Froude numbers to describe the dynamical characteristics of vehicles.

Output Power Spectra and Vehicle Response

It will be shown subsequently that the calculation of the absorbed power and total power of the driver requires the output acceleration and velocity power spectra. The power spectra of the vertical motion of a point on a vehicle can be obtained from equation (208) and equations (198) through (202) to be

$$P_{do}(\Omega) = |T_{dd}|^2 e^{-F} P_d(\Omega) \quad (252)$$

$$P_{vo}(\Omega) = (2\pi u \Omega)^2 |T_{dd}|^2 e^{-F} ASW(2) P_d(\Omega) \quad (253)$$

$$P_{ao}(\Omega) = (2\pi u \Omega)^4 |T_{dd}|^2 e^{-F} ASW(4) P_d(\Omega) \quad (254)$$

The vehicle speed enters directly in equations (253) and (254), but the dependence on the vehicle speed is also indirectly introduced through the

transmission function, as for instance in equation (214). The corresponding power spectra expressed in terms of the time frequency are obtained using equation (154) to be

$$P'_{do}(f) = |T_{dd}|^2 e^{-F} P'_d(f) \quad (255)$$

$$P'_{vo}(f) = (2\pi f)^2 |T_{dd}|^2 e^{-F} ASW^{(2)} P'_d(f) \quad (256)$$

$$P'_{ao}(f) = (2\pi f)^4 |T_{dd}|^2 e^{-F} ASW^{(4)} P'_d(f) \quad (257)$$

The standard deviations of the vertical displacement, velocity, acceleration and absorbed power at a point on the vehicle can be calculated from integrals of the output power spectra, given by equations (252) - (254), over the frequency ranges of the five basic types of roughness power spectra. Equations (252) - (254) show that P_{do} and P_{vo} diverge for $f = 0$ (or $\Omega = 0$). This is identically the same problem that was encountered in the roughness models of Parts I and II where it was shown that $P_d(\Omega)$ diverge for $\Omega = 0$. Therefore the same difficulties that appear in the roughness models of spectral types 1, 2 and 5 appear in the vehicle response problem. Equations (254) and (257) show that $P_{ao}(\Omega)$ and $P'_{ao}(f)$ are not divergent for $\Omega = 0$, corresponding to the situation that $P_c(\Omega)$ is not divergent for $\Omega = 0$ as described in Part II.

The divergent integrals resulting from the calculation of the RMS values of the output vertical displacement and velocity can be evaluated in inserting a filter function similar to that defined in equation (6). Thus the following integration factor can be used

$$\phi^{-2} = \frac{(2\pi\gamma^1\Omega)^4}{[1 + (2\pi\gamma^1\Omega)^2]^2} \quad (258)$$

where γ^1 = filter constant. This integration factor is not necessary for the calculation of absorbed power because this calculation involves only the acceleration power spectrum.

The standard deviations of the vehicle displacement, velocity and acceleration are given by

$$\sigma_{do}^2 = \int_0^\infty P_{do}(\Omega) \phi^{-2} d\Omega = \int_0^\infty P'_{do}(f) \phi^{-2} df \quad (259)$$

$$\sigma_{vo}^2 = \int_0^\infty P_{vo}(\Omega) \phi^{-2} d\Omega = \int_0^\infty P'_{vo}(f) \phi^{-2} df \quad (260)$$

$$\sigma_{ao}^2 = \int_0^{\infty} P_{ao}(\Omega) d\Omega = \int_0^{\infty} P'_{ao}(f) df \quad (261)$$

The integrals in equation (259) through (261) are evaluated only in the regions for which the power spectra are positive.

Absorbed Power and Six Watt Speed Calculated by Power Spectrum Method

The absorbed power is related to the vertical acceleration of the driver (at the drivers seat) and is defined in terms of the vertical acceleration power spectrum as follows⁶

$$A_p = \int_0^{\infty} H_a^2(f) P'_{ao}(f) df = \int_0^{\infty} A'_p(f, u) df \quad (262)$$

where

A_p = absorbed power (watts)

$H_a(f)$ = human factor function $[\sqrt{\text{watts}/(\text{ft}/\text{sec}^2)}]$

$P'_{ao}(f)$ = output vertical acceleration power spectrum at the location of the drivers seat

$A'_p(f, u)$ = absorbed power spectral function

The human factor function $H_a(f)$ is empirically determined and has the form of a band pass filter.⁶ This function appears in Figure 9e.

The frequency dependence of the absorbed power is given by equations (254), (257) and (262) as

$$A_p(\Omega, u) = (2\pi u \Omega)^4 |T_{dd}|^2 e^{-F} H_a^2 ASW^{(4)} P_d(\Omega) \quad (263)$$

$$A'_p(f, u) = (2\pi f)^4 |T_{dd}|^2 e^{-F} H_a^2 ASW^{(4)} P'_d(f) \quad (264)$$

where $A_p(\Omega, u) = u A'_p(f, u)$. Equations (262) and (264) show that five basic quantities enter into the absorbed power calculation, and these depend on the vehicle dynamics, vehicle geometry, driver location and terrain roughness:

- a. transmission function
- b. low pass filter associated with the ground contact length
- c. human factor function

d. curvature spectral window function for vehicle

e. power spectrum of terrain elevation

The roughness power spectrum is given by the three parameter model, and refers to actual terrain described by the parameters C, D and E of Part II.

Because the functions T_{dd} and H_a that appear in equations (263) and (264) are intrinsically functions of the time frequency f , while the functions e^{-F} and $ASW^{(4)}$ are intrinsically functions of the spatial frequency Ω , it follows from $f = u\Omega$ that the absorbed power given by equation (262) always depends on the vehicle speed. The six watt vehicle speed is obtained from the absorbed power equation (262) by taking $A_p = 6$ watts.

It should be pointed out that the absorbed power dissipated by the driver is not the same as the total power associated with the kinetic and potential energies of the motion of the driver. The RMS value of the total power delivered to the driver is given by

$$\sigma_{po} = \frac{W_D}{g} \sqrt{\int_0^\infty P_{vo}(\Omega) P_{ao}(\Omega) d\Omega} \quad (265)$$

where

σ_{po} = RMS value of total power of driver

W_D = weight of driver

A comparison of the experimental values of absorbed power with values predicted by the numerical integration of equations (262) and (264) are shown in Figures 10a through 11c for a series of track laying vehicles. Figure 11d gives a comparison between predicted and measured values of the six watt speed for track laying vehicles. A similar procedure for trucks appears in Figures 12a through 12d.

Linear Regression Prediction of the Six Watt Speed

The six watt speed is the vehicle speed at which the driver is absorbing six watts of power; it is a measure of ride quality. A high value for the six watt speed means a smooth ride, and a low value means a rough ride. The value of the six watt speed depends on both terrain and vehicle characteristics.

For the purpose of the design and testing of vehicles, it is important to have a simple expression for the six watt speed giving its dependence on terrain roughness parameters and on vehicle parameters. In this way the results of vehicle tests conducted at different terrain areas with different types of vehicles can be compared, and an evaluation of design changes can be made. The vehicle parameters describe the geometry and internal dynamics, while the

terrain parameters describe the displacement, slope and curvature of an elevation profile.

Values of the six watt speed for several vehicles have been measured for a number of terrain sites where elevation profiles have been determined. The regression analysis given here represents the six watt speed as simple powers of the terrain roughness parameters and the vehicle parameters. This analysis is valid only if the six watt speed is a monotonically increasing or decreasing function of the chosen parameters. It was found that the vehicle dynamics parameters k , m and C could not be successfully brought into the regression analysis, and therefore only terrain roughness and vehicle geometry were considered.

A regression analysis incorporating k , m and C could not be accomplished because the dependence of the six watt speed of these parameters could not be represented by a simple power law. The dependence on the vehicle weight, for example, was found to be either direct or inverse depending on the choice of the resonance frequency or the damping ratio as a basic vehicle dynamics parameter; both choices gave essentially the same quality of fit to the measured six watt speeds. This suggests that the dependence of the six watt speed on the vehicle weight is more complicated than a simple power law. In fact, the six watt speed is expected to initially increase with the vehicle weight producing a smoother ride, and then decrease with additional weight giving a rougher ride due to hitting the bump stops.

It is possible to find a direct correlation between the six watt speed, the three terrain roughness descriptors σ_d , σ_s and σ_c for detrended data, and the vehicles parameters. Both wheeled vehicles and track laying vehicles were considered for this study.

Track Laying Vehicles

Seven mathematical forms were chosen for the regression analysis of the six watt speed for track laying vehicles. They are as follows:

$$u_6 = A\sigma_d^\alpha \quad (266)$$

$$u_6 = A\sigma_s^\beta \quad (267)$$

$$u_6 = A\sigma_c^\gamma \quad (268)$$

$$u_6 = A\sigma_d^\alpha T_L^\delta \quad (269)$$

$$u_6 = A\sigma_d^\alpha J_L^\eta \quad (270)$$

$$u_6 = A \sigma_d^\alpha T_L^\delta J_L^\eta \quad (271)$$

$$u_6 = A \sigma_d^\alpha \sigma_s^\beta \sigma_c^\gamma T_L^\delta J_L^\eta \quad (272)$$

where

u_6 = six watt speed of vehicle

$\sigma_d, \sigma_s, \sigma_c$ = RMS values of displacement, slope and curvature, respectively, of a detrended elevation profile ($\lambda = 10$ ft)

T_L = track length

J_L = jounce length

The coefficients in equations (266) through (272) were obtained by fitting these equations to measured six watt speeds. Eight track laying vehicles were used in this analysis, LEO 2AV, M60 A1, ATR, SM1, AISV, HIMAG-5, MICV and the M113. The six watt speed was measured for these vehicles for a total of twenty-four terrain sites. The dimensions of the quantities shown in equations (266) through (272) are chosen to be as follows: $[u_6] = \text{mph}$, $[\sigma_d] = \text{in}$, $[\sigma_s] = 1$, $[\sigma_c] = \text{in.}^{-1}$, $[T_L] = \text{in}$. and $[J_L] = \text{in}$.

This data combined with a library regression computer program gave the following results for the six watt speed and the coefficient of fit (cf):

$$u_6 = \frac{23.55}{\sigma_d^{0.50}} \quad (266a)$$

$$cf = 0.29$$

$$u_6 = \frac{9.62}{\sigma_s^{0.190}} \quad (267a)$$

$$cf = 0.02$$

$$u_6 = \frac{47.2}{\sigma_c^{0.211}} \quad (268a)$$

$$cf = 0.04$$

$$u_6 = \frac{0.393 T_L^{0.874}}{\sigma_d^{0.875}} \quad (269a)$$

$$cf = 0.70$$

$$u_6 = \frac{3.33 J_L^{0.98}}{\sigma_d^{0.85}} \quad (270a)$$

$$cf = 0.82$$

$$u_6 = \frac{1.324 T_L^{0.289} J_L^{0.761}}{\sigma_d^{0.897}} \quad (271a)$$

$$cf = 0.84$$

$$u_6 = \frac{0.944 \sigma_s^{0.708} T_L^{0.412} J_L^{0.672}}{\sigma_d^{1.20} \sigma_c^{0.407}} \quad (272a)$$

$$cf = 0.86$$

Equations (266a) through (268a) show that the detrended displacement σ_d is the relevant terrain roughness parameter for track laying vehicles, while σ_s and σ_c play secondary roles. Equations (269a) through (271a) show that the jounce length J_L is the primary vehicle parameter for track laying vehicles while the track length T_L plays a secondary role. The best fit to the measured six watt speed data is given by equation (272a) with all parameters included, but the fit is not much better than given by equation (270a) with only the two parameters σ_d and J_L . A comparison between the experimental six watt speed and those predicted by equation (272a) is shown in Figure 13a.

When the vehicle dynamics parameters k , m and C are eventually brought into the expression for u_6 , they should be entered as nondimensional parameters in the form of the damping ratio and the Froude numbers.¹⁷

Wheeled Vehicles

Seven mathematical forms were chosen for the analysis of the six watt speed for wheeled vehicles. They are expressed in terms of the tire radius (T_R) and wheel base length (L_{WB}) as follows:

$$u_6 = A \sigma_d^\alpha \quad (273)$$

$$u_6 = A \sigma_c^\gamma \quad (274)$$

$$u_6 = A \sigma_s^\beta \quad (275)$$

$$u_6 = A \sigma_s^\alpha L_{WB}^\delta \quad (276)$$

$$u_6 = A \sigma_s T_R^\epsilon \quad (277)$$

$$u_6 = A \sigma_s^\alpha L_{WB}^\delta T_R^\epsilon \quad (278)$$

$$u_6 = A \sigma_d^\alpha \sigma_s^\beta \sigma_c^\gamma L_{WB}^\delta T_R^\epsilon \quad (279)$$

The coefficients in equations (273) through (279) were obtained by fitting these equations to measured six watt speeds for trucks. Five trucks were used in this analysis: PAC-CAR, TARADCOM-HMTT, 10 ton (8x8) - Cargo truck A; DRAGON WAGON, 10 ton (8x8) - Cargo truck B; GERMAN MAN, 10 ton (8x8) - Cargo truck C; M656, 5 ton (8x8); M520E1 GOER, 8 ton (4x4); and the Czechoslovakian TATRA 813.

A library regression routine (MULFIT) was used to analyze the six watt speed data for these five trucks, and gave the following results for the six watt speed and the coefficient of fit (cf):

$$u_6 = \frac{14.87}{\sigma_d^{0.544}} \quad (273a)$$

$$cf = 0.38$$

$$u_6 = \frac{0.0411}{\sigma_c^{1.12}} \quad (274a)$$

$$cf = 0.51$$

$$u_6 = \frac{0.789}{\sigma_s^{0.996}} \quad (275a)$$

$$cf = 0.62$$

$$u_6 = \frac{1285}{\sigma_s^{0.996} L_{WB}^{1.415}} \quad (276a)$$

$$cf = 0.76$$

$$u_6 = \frac{217.9}{\sigma_s^{0.966} T_R^{1.742}} \quad (277a)$$

$$cf = 0.80$$

$$u_6 = \frac{317.7}{\sigma_s^{0.996} L_{WB}^{0.166} T_R^{1.59}} \quad (278a)$$

$$cf = 0.80$$

$$u_6 = \frac{1099 \sigma_d^{0.475} \sigma_c^{0.942}}{\sigma_s^{2.22} L_{WB}^{0.166} T_R^{1.59}} \quad (279a)$$

$$cf = 0.82$$

Equations (273a) through (275a) show that the detrended slope σ_s is the significant terrain roughness parameter for wheeled vehicles, while σ_c and σ_d play subordinate roles. The best fit to the measured six watt speeds^c of wheeled vehicles is given by equation (279a) with all variables included, but this fit is not much better than shown in equation (277a) with only two parameters σ_s and T_R . A comparison between the experimental values of the six watt speed and those^R predicted by equation (279a) is given in Figure 13b. The relatively poor agreement shown in Figure 13b suggests that an alternative vehicle parameter, such as the jounce length, is required to obtain a better correlation between measured and predicted six watt speeds for wheeled vehicles.

Dimensional Analysis

Dimensional analysis uses relationships between nondimensional quantities which remain valid irrespective of the scale of the physical system.¹⁷ The procedure is to calculate a set of relevant dimensionless parameters for a physical system. For this study the physical system is a vibrating vehicle moving over rough terrain.

The Froude numbers for a physical system are given by¹⁷

$$\xi = \frac{MV^2}{FL} \quad (280)$$

where ξ = Froude number, M = characteristic mass, V = characteristic speed, F = characteristic forces operating in the system, and L = characteristic length.

The Froude numbers associated with a linear harmonic oscillator are

$$\xi_1 = \frac{MV^2}{KL} \sim \frac{V^2}{f_R^2 L} = \left(\frac{V}{f_R L} \right)^2 \quad (281)$$

$$\xi_2 = \frac{MV^2}{CVL} = \frac{MV}{CL} \quad (282)$$

where f_R = resonance frequency of vehicle, K = spring constant of vehicle, and C = damping constant of vehicle. Because the resonance frequency of a vehicle is a directly measurable quantity, equation (281) is used as the appropriate Froude number and therefore the appropriate dimensionless parameter for representing the six-watt speed for vehicles is

$$\xi_{u_6} = \frac{u_6}{f_R T_L} \quad (283)$$

For wheeled vehicles the characteristic lengths would be the tire radius and wheelbase length. The other dimensionless parameter for a vibrating system is the damping ratio

$$\xi_D = \frac{C}{2\sqrt{KM}} \quad (284)$$

A third parameter that was examined is the ratio of jounce length to ground contact length

$$\xi_L = J_L/T_L \quad (285)$$

For a vibration problem it is the vehicle mass $M = W/g$ that enters (281) through (284) not the vehicle weight. Dimensionless parameters such as $W/(KL)$ and $W/(CV)$ are inappropriate for a vibration problem. The correct dimensionless parameters equivalent to (283) are $MV/(CL)$ and $CV/(KL)$. This can be seen from the extreme case of zero gravity where $g = 0$ and $W = 0$ but $M =$ some fixed value; in this case vibrations can still occur. On the other hand for a statics problem, such as deformation of a solid (vehicle) under the action of gravity, it is the weight and not the mass that enters the appropriate dimensionless parameters.

Terrain roughness has been described by the three parameters σ_d , σ_c and σ_s . Within this description the terrain roughness dimensionless parameters are

$$\xi_s = \sigma_s \quad (286)$$

$$\xi_{cd} = \sigma_c \sigma_d \quad (287)$$

A combination of these parameters that was examined is

$$\xi_R = \frac{\sigma_s}{\sigma_c \sigma_d} \quad (288)$$

A number of dimensionless relationships were developed with corresponding coefficients of fit from data for eight track laying vehicles, and are as follows

$$\xi_{u_6} = 0.011 \xi_R^{1.28} \quad (289)$$

$$cf = 0.60$$

$$\xi_{u_6} = \frac{0.012 \xi_R^{1.21}}{\xi_D^{0.248}} \quad (290)$$

$$cf = 0.70$$

$$\xi_{u_6} = \frac{0.027 \xi_S^{2.06}}{\xi_D^{0.23} \xi_{cd}^{1.57}} \quad (291)$$

$$cf = 0.74$$

$$\xi_{u_6} = \frac{0.025 \xi_S^{2.06}}{\xi_D^{0.23} \xi_{cd}^{1.57} \xi_L^{0.02}} \quad (292)$$

$$cf = 0.74$$

Equation (292) shows an insignificant dependence on the ratio of jounce length to track length. A comparison of measured values of $u_6/(f_R T_L)$ with those values if shown predicted by equation (291) is shown in Figure 13c.

PART VI: CONCLUSIONS

CONCLUSIONS. This paper generalizes the method of characterizing the ground surface displacement profile by a one parameter power spectrum of the form $C\Omega^{-2}$. A three parameter model of the power spectrum of the terrain displacement profile data is introduced in such a manner that the additional parameters will more accurately describe the contribution of the long wavelengths to the surface roughness, and will describe the cases where periodicities are present in the terrain such as in the case of plowed fields.

The three roughness power spectrum parameters are used to calculate the power spectra and standard deviation values of the vertical displacement, velocity, acceleration and power absorbed by the driver for a vehicle operating on rough terrain. A comparison of theoretical and experimental results was made.

The theoretical and experimental studies of terrain roughness and dynamic vehicle response yields the following conclusions:

- a. A three parameter power spectrum model can be used to classify terrain roughness into five basic types which adequately describe natural and manmade terrain features including periodicities (Parts I and II).
- b. The three parameters of the roughness power spectrum can be determined from the standard deviations of the displacement, slope and curvature of a detrended elevation profile, but in some cases undetrended data can be used (Part II).
- c. The power absorbed by the driver of a vehicle depends on:
(1) the human factor function relating absorbed power to the acceleration power spectrum, (2) the vehicle transmission function that describes the internal dynamics of a vehicle, (3) the low pass ground contact length filter that describes the filtering effect of a track or wheel, (4) the vehicle spectral window functions that introduce the geometry of the vehicle-ground contact, and (5) the three parameter roughness power spectrum that introduces surface roughness (Parts III, IV and V).
- d. The six watt speed for track laying vehicles can be related by a regression analysis to the vehicle geometry and the three roughness descriptors σ_d , σ_s and σ_c for detrended data. The significant terrain roughness parameter for track laying vehicles is σ_d , while for wheeled vehicles it is σ_s (Part V).

ACKNOWLEDGEMENT. I wish to thank N. R. Murphy, Jr., C. J. Nuttall, Jr., D. D. Randolph and B. G. Schreiner for their helpful advice. The computer program RRFN was developed by R. B. Ahlvin.

LITERATURE CITED

1. Weiss, R., "Characterization of Terrain Roughness, Volume I, Microroughness Description and Its Application to the Dynamic Response of Vehicles," Draft Report, Sep 1980, U. S. Army Engineer Waterways Experiment Station, CE, Vicksburg, MS.
2. Van Deusen, R. D., "A Statistical Technique for the Dynamic Analysis of Vehicles Traversing Rough Yielding and Non-yielding Surfaces," Contract Report No. NASW-1287, May 1966, Advanced Projects Organization, Chrysler Corp, Detroit, MI.
3. Blackman, R. B. and Tukey, J. W., The Measurement of Power Spectra, Dover Publications, New York, 1958.
4. Bendat, J. S. and Piersol, A. G., Random Data: Analysis and Measurement Procedures, Wiley-Interscience, New York, 1971.
5. Bekker, M. G., Introduction to Terrain-Vehicle Systems, University of Michigan Press, Ann Arbor, 1969.
6. Lins, William F., "Human Vibration Response Measurement," Technical Report No. 11551, June 1972, U. S. Army Tank Automotive Command, Warren, MI.
7. Pradko, F., Lee, R. and Kaluza, V., "Theory of Human Vibration Response," presented at the Winter Annual Meeting and Energy Systems Exposition of the American Society of Mechanical Engineers, New York, NY, 27 Nov-1 Dec 1966.
8. Schreiner, B. G., "Ride and Shock Test Results for the Leopard 2 AV Tank," Miscellaneous Paper M-77-3, Mar 1977, U. S. Army Engineer Waterways Experiment Station, CE, Vicksburg, MS.
9. _____, "Ride and Shock Test Results for the M60A1, XM-1 Chrysler, and XM-1 General Motors Tanks."
10. Schreiner, B. G. and Randolph, D. D., "Ride and Shock Test Results and Mobility Assessment of Czechoslovakia Tatra 813, U. S. M520E1 GOER, and U. S. M656 Cargo Trucks," Technical Report GL-79-9, July 1979, U. S. Army Engineer Waterways Experiment Station, CE, Vicksburg, MS.
11. _____, "Ride and Shock Test Results and Mobility Assessment of German M.A.N., U. S. M520E1 GOER, and U. S. M656 Cargo Trucks," Technical Report GL-79-17, Sept 1979, U. S. Army Engineer Waterways Experiment Station, CE, Vicksburg, MS.
12. _____, "Ride and Shock Test Results and Mobility Assessment of Selected 10-Ton Cargo Trucks," Technical Report GL-79-5, May 1979, U. S. Army Engineer Waterways Experiment Station, CE, Vicksburg, MS.

13. Robinson, J. H. Randolph, D. D. and Schreiner, B. G., "Ride and Shock Test Results and Mobility Assessment of Selected 1/4- to 1-1/4-Ton Vehicles," Technical Report GL-79-3, Mar 1979, U. S. Army Engineer Waterways Experiment Station, CE, Vicksburg, MS.
14. Jacobsen, L. S. and Ayre, R. S., Engineering Vibrations, McGraw-Hill Book Co., New York, 1958.
15. Snowdon, J. C., Vibration and Shock in Damped Mechanical Systems, John Wiley, New York, 1968.
16. Crafton, P. A., Shock and Vibration in Linear Systems, Harper & Brothers, New York, 1961.
17. Duncan, W. J., Physical Similarity and Dimensional Analysis, Edward Arnold and Co., London, 1953.

Table 1'
Units of the Power Spectra

C	in.
D	dimensionless
E	in. ⁻¹
$P_d(\Omega)$	in. ³
$P'_d(f)$	in. ² sec
$P_v(\Omega)$	in. ³ sec ⁻²
$P'_v(f)$	in. ² sec ⁻¹
$P_a(\Omega)$	in. ³ sec ⁻⁴
$P'_a(f)$	in. ² sec ⁻³
$P_s(\Omega)$	in.
$P'_s(f)$	sec ⁻¹
$P_c(\Omega)$	in. ⁻¹
$P'_c(f)$	in. ⁻² sec

Table 2
Calculated Values of the Roughness Power Spectrum Coefficients

PROFILE ID	LOCATION	DETRENDED ($\lambda=10$ ft)			$D, 10^{-5}$	$E, 10^{-8} \text{ in}^{-1}$	$\Omega_0, 10^{-3} \text{ in}^{-1}$	$\Omega_1, 10^{-3} \text{ in}^{-1}$	SPECTRUM TYPE
		$\sigma_d, \text{ in}$	σ_s	$\sigma_c, \text{ in}^{-1}$					
AISV1	Huntsville, Alabama	1.32	.049	.0053	0.8952	-0.5426	0.4876	-	3
AISV2		0.57	.038	.0043	0.6596	-0.4364	0.7987	-	3
AISV3		0.72	.031	.0033	0.3188	-0.3299	0.6264	-	3
AISV4AT		0.57	.032	.0042	0.8920	0.2464	0.8396	4.611	5
FTKCTA1	Ft Knox, Kentucky	2.03	.048	.0046	0.4125	-0.1924	0.1205	-	3
FTKCTA2		5.53	.088	.0058	-1.469	1.837	60.73	-	2
FTKSTV1		4.84	.106	.0069	-3.027	-5.945	0.3763	52.19	4
FTKSTV4		1.70	.083	.0061	-1.541	-7.370	0.7405	64.58	4
FTKSTV9		3.26	.078	.0063	-0.4240	-2.461	0.3654	158.6	4
SR1LT82	Ft Knox, Kentucky	0.59	.031	.0035	0.4388	-0.2434	0.6957	-	3
SR1RT82		0.54	.026	.0027	0.1871	-0.3040	0.6962	-	3
SR2LT83		0.78	.030	.0035	0.4937	-0.0248	0.1666	-	3
SR2RT83		1.06	.037	.0038	0.3689	-0.4369	0.5112	-	3
SR4LT83		3.38	.075	.0051	-1.325	-2.850	0.3740	57.53	4
SR4RT83		3.33	.074	.0047	-1.591	-3.157	0.3992	49.70	4
SR5LT83		2.63	.065	.0059	0.3615	-1.068	0.2939	-	3
SR5RT83		2.27	.047	.0033	-0.4325	-0.7725	0.2753	64.87	4
HOOD1DM	Ft Hood, Texas	0.51	.026	.0029	0.2900	-0.1887	0.6874	-	3
HOOD2DM		1.39	.104	.0139	10.00	2.783	0.6948	4.00	5
HOOD3DM		1.91	.078	.0082	1.874	-2.135	0.6040	-	3
HOOD1T(T1N)		1.56	.078	.0092	3.445	-0.6377	0.5827	-	3
HOOD2TX		0.94	.046	.0055	1.275	-0.1139	0.4735	-	3
HOOD3T(3TH)		0.57	.026	.0030	0.3472	-0.0950	0.5477	-	3
HOOD4T(T4M)		1.23	.039	.0042	0.5681	-0.1959	0.2956	-	3
SRIHE1M		0.42	.023	.0023	0.1060	-0.3063	0.7459	-	3

Table 2 (Continued)

PROFILE ID	LOCATION	DETRENDED ($\lambda=10$ ft)			$C, 10^{-3} \text{ in}$	$D, 10^{-5}$	$E, 10^{-8} \text{ in}^{-1}$	$\Omega_0, 10^{-3} \text{ in}^{-1}$	$\Omega_1, 10^{-3} \text{ in}^{-1}$	SPECTRUM TYPE
		$\sigma_d, \text{ in}$	σ_s	$\sigma_c, \text{ in}^{-1}$						
T21	Hi Mag	0.73	.038	.0038	0.291	1.092	-0.815	0.732	-	3
T24	Courses,	1.07	.048	.0047	0.387	1.850	-1.290	0.687	-	3
T22	Pt Knox,	1.89	.129	.0147	7.874	5.247	-4.755	0.808	-	3
T13	(Right Track)	3.41	.084	.0061	-1.337	9.279	-4.145	0.450	68.93	4
T14	"	5.15	.104	.0053	-4.413	17.53	-6.144	0.354	39.36	4
T38C	"	0.79	.038	.0040	0.440	0.839	-0.600	0.691	-	3
T36	"	1.02	.039	.0039	0.325	1.086	-0.665	0.602	-	3
T30	"	1.98	.071	.0052	-1.078	7.151	-4.684	0.662	65.70	4
T32	"	3.68	.088	.0059	-1.999	11.01	-4.922	0.451	54.64	4
T33	"	2.36	.052	.0038	-0.454	3.377	-1.117	0.332	74.05	4
E1	"	0.79	.033	.0031	0.109	0.992	-0.671	0.672	-	3
E3	"	0.97	.036	.0035	0.213	1.028	-0.626	0.601	-	3
E5	"	1.62	.048	.0039	-0.196	2.715	-1.478	0.547	137.7	4
E7	"	3.50	.078	.0047	-1.998	9.246	-3.817	0.417	45.85	4
E9	"	2.31	.050	.0039	-0.240	2.810	-0.745	0.266	116.8	4
APG38	APG, MD	2.65	.113	.0088	-2.00	17.120	-12.020	0.707	84.60	4
APG40	"	1.04	.045	.0051	0.96	0.596	-0.350	0.541	-	3
APG41	"	0.47	.027	.0034	0.51	-0.035	0.0046	0.175	0.512	5
APG42	"	1.18	.092	.0112	5.38	0.896	-0.950	0.946	-	3
APG43	"	0.30	.018	.0024	0.30	-0.167	0.113	0.795	4.68	5
APG44	"	3.93	.082	.0057	-1.42	8.830	-2.6300	0.299	61.70	4
APG29	"	2.15	.096	.0111	4.74	1.999	-1.152	0.514	-	3
APG31	"	3.18	.076	.0059	-0.71	6.978	-2.764	0.398	98.44	4
APG32	"	1.95	.0490	.0045	0.27	1.963	-0.571	0.290	-	3
APG34	"	1.55	.080	.0103	5.31	-1.949	1.422	1.005	2.661	5
APG36	"	3.71	.075	.0064	0.24	4.822	-0.023	0.0047	-	3
APG37	"	0.83	.032	.0038	0.64	0.018	0.075	-	-	1

Table 3

Comparison of Detrended and Undetrended Methods for a Type 3 Roughness Spectrum

PROFILE ID	DETRENDED SCHEME					UNDETRENDED SCHEME						
	$\sigma_d \cdot$ in	σ_s	σ_c in ⁻¹	C 10 ⁻³ in	D 10 ⁻⁵	E 10 ⁻⁸ in ⁻¹	σ_d in	σ_s	σ_c in ⁻¹	C 10 ⁻³ in	D 10 ⁻⁵	E 10 ⁻⁸ in ⁻¹
APG48LT	1.39	0.045	0.0049	0.80	0.79	-0.23	23.57	0.053	0.0055	1.21	0.351	-0.011
APG52RT	0.96	0.033	0.0034	0.30	0.65	-0.33	1.91	0.038	0.0036	0.31	0.81	-0.53
APG52LT	1.03	0.039	0.0042	0.55	0.71	-0.38	3.58	0.045	0.0045	-0.68	0.63	-0.20
APG53RT	1.42	0.053	0.0049	0.22	2.62	-1.66	3.79	0.060	0.0052	0.43	2.32	-1.24
APG53LT	1.25	0.053	0.0048	0.12	2.84	-1.85	3.13	0.059	0.0052	0.40	2.43	-1.62
APG56RT	2.25	0.046	0.0040	0.108	1.82	-0.05	8.54	0.058	0.0042	0.125	1.97	-0.42
APG56LT	1.83	0.039	0.0034	0.072	1.34	-0.15	3.74	0.048	0.0035	-0.06	1.86	-0.87

Table 4
Dynamical Parameters of Track Vehicles

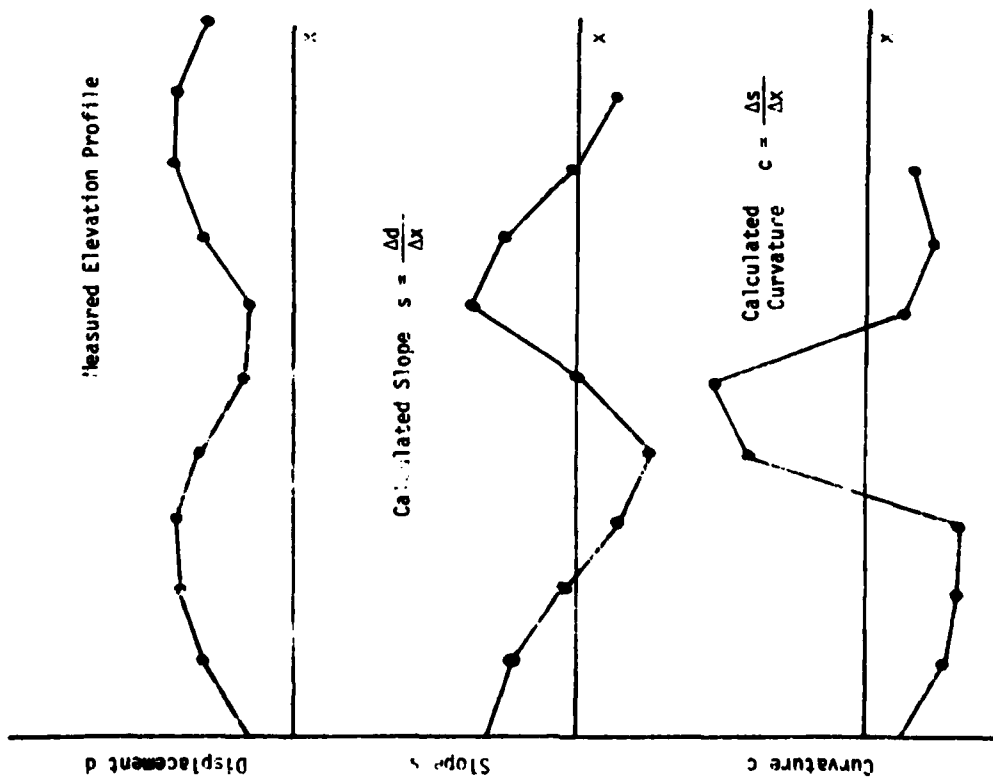
<u>Vehicle Type</u>	<u>Weight lb</u>	<u>Spring Constant lb/in.</u>	<u>Damping Constant lb sec/in.</u>	<u>Track Length in.</u>
M113A1	24,200	6,060	3110	105
MICV	43,000	8,400	720	150
AISV	2,940	300	80	50.25
HIMAG-5	79,910	10,000	400	168
LEO 2AV	111,000	15,750	8000	188.3
M60 A1	106,000	20,000	8000	171

Table 5
Dynamical Parameters for Trucks

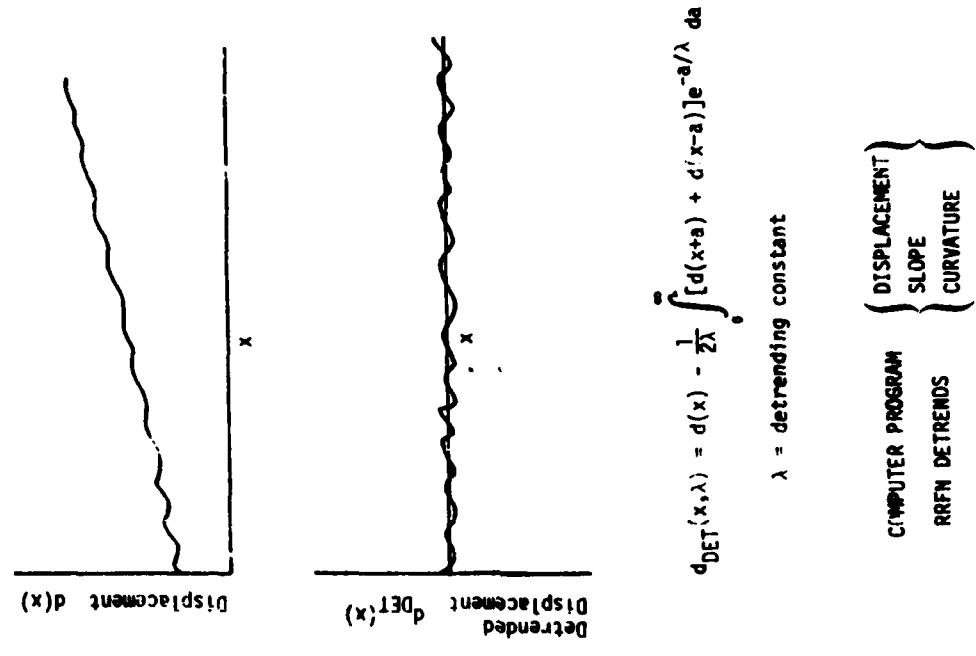
Vehicle Type	Body			Wheel Assembly		
	Weight lb	Spring lb/in.	Damping lb sec/in.	Weight lb	Spring Constant lb/in.	Damping Constant lb sec/in.
PAC-CAR TARADCOM-HMTT 10 ton (8x8)	46,179	4718	830	5131	75,490	830
DRAGON WAGON 10 ton (8x8)	44,136	4509	822	4904	72,150	822
GERMAN MAN 10 ton (8x8)	47,610	4864	887	5290	77,829	887
M656 5 ton (8x8)	23,040	2354	250	2560	37,664	250
M520E1-GOER 8 ton (4x4)	41,400	2500	1000	--	--	--

Table 6
Geometrical Properties of Trucks

Vehicle Type	Tire Radius in.	L ₁₂ in.	L ₁₃ in.	L ₁₄ in.	L ₂₃ in.	L ₂₄ in.	L ₃₄ in.
PAC-CAR TARADCOM-HMTT 10 ton (8x8)	26	58	190	248	132	190	58
DRAGON WAGON 10 ton (8x8)	26	58	202	260	144	202	58
GERMAN MAN 10 ton (8x8)	23.75	65.5	209.5	275	144	209.5	65.5
M656 5 ton (8x8)	22	56.25	147.75	204	91.5	147.75	56.25
M520E1-GOER 8 ton (4x4)	34.5	235	--	--	--	--	--

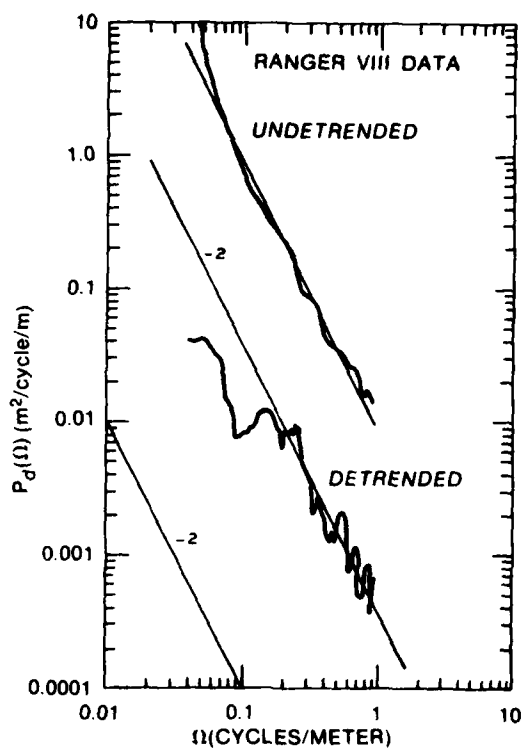


a.

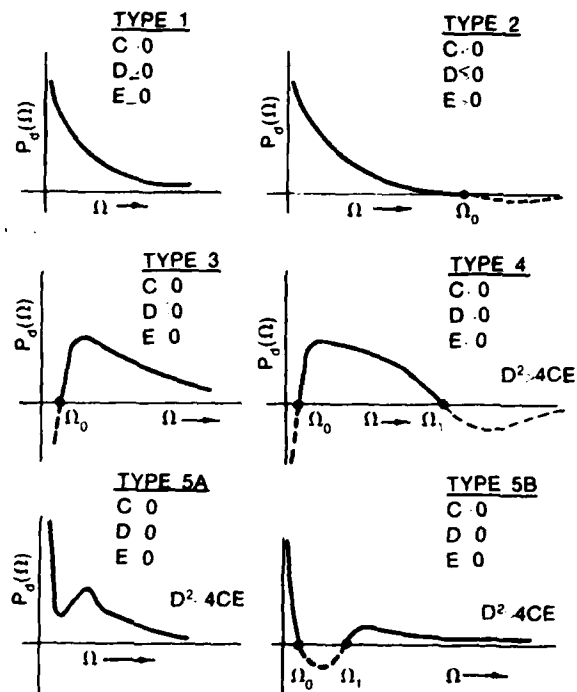


b.

Figure 1



a



b

COMPLEX INTEGRATION CONTOURS



INTEGRATION PATH EVALUATING INTEGRALS

$$g_1(\lambda), g_3(\lambda)$$

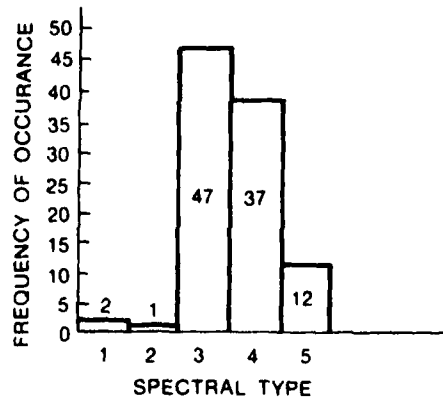
$$h_1(\lambda), h_3(\lambda)$$



INTEGRATION PATH EVALUATING INTEGRALS

$$g_2(\lambda), h_2(\lambda)$$

c



d

Figure 2

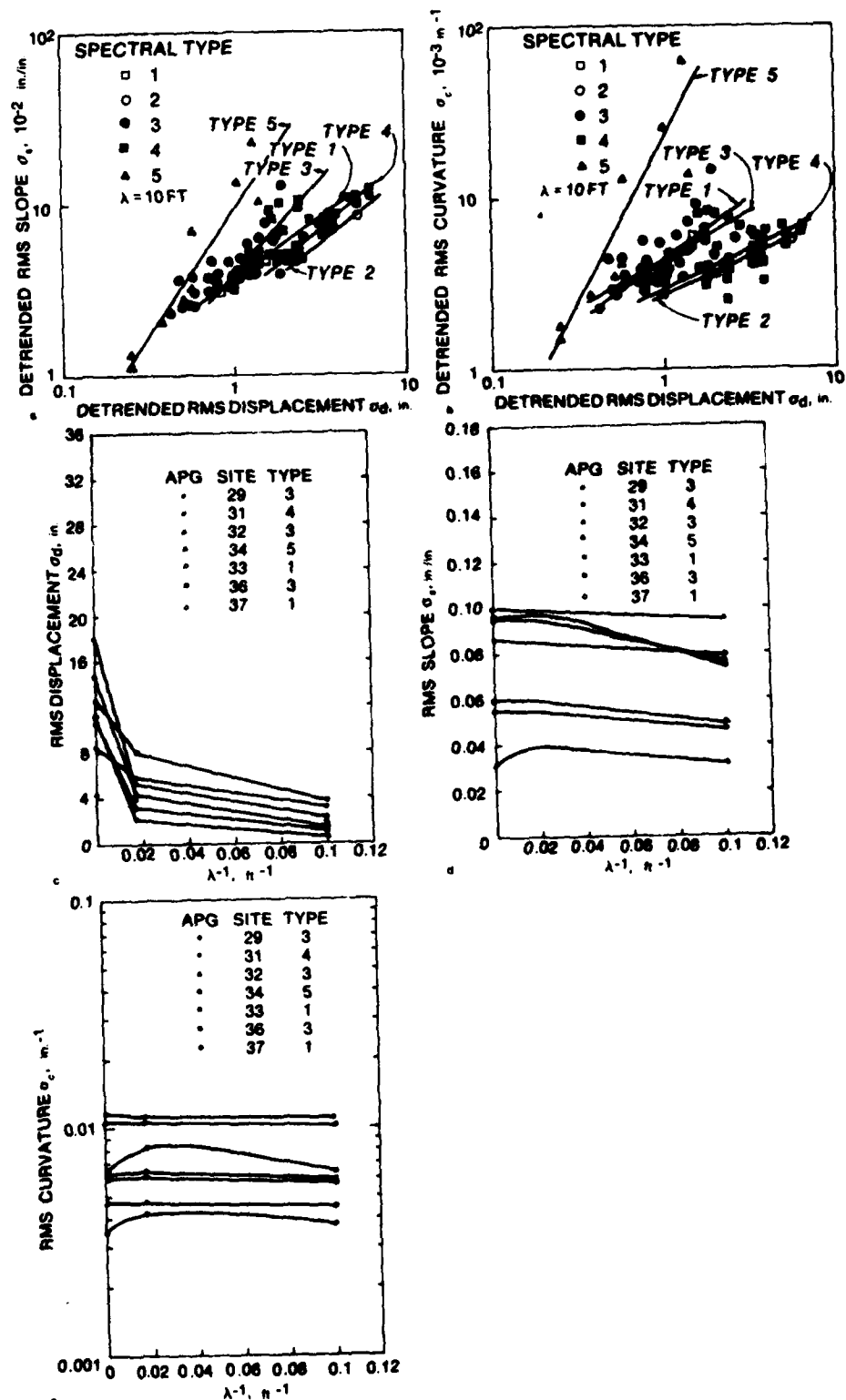


Figure 3

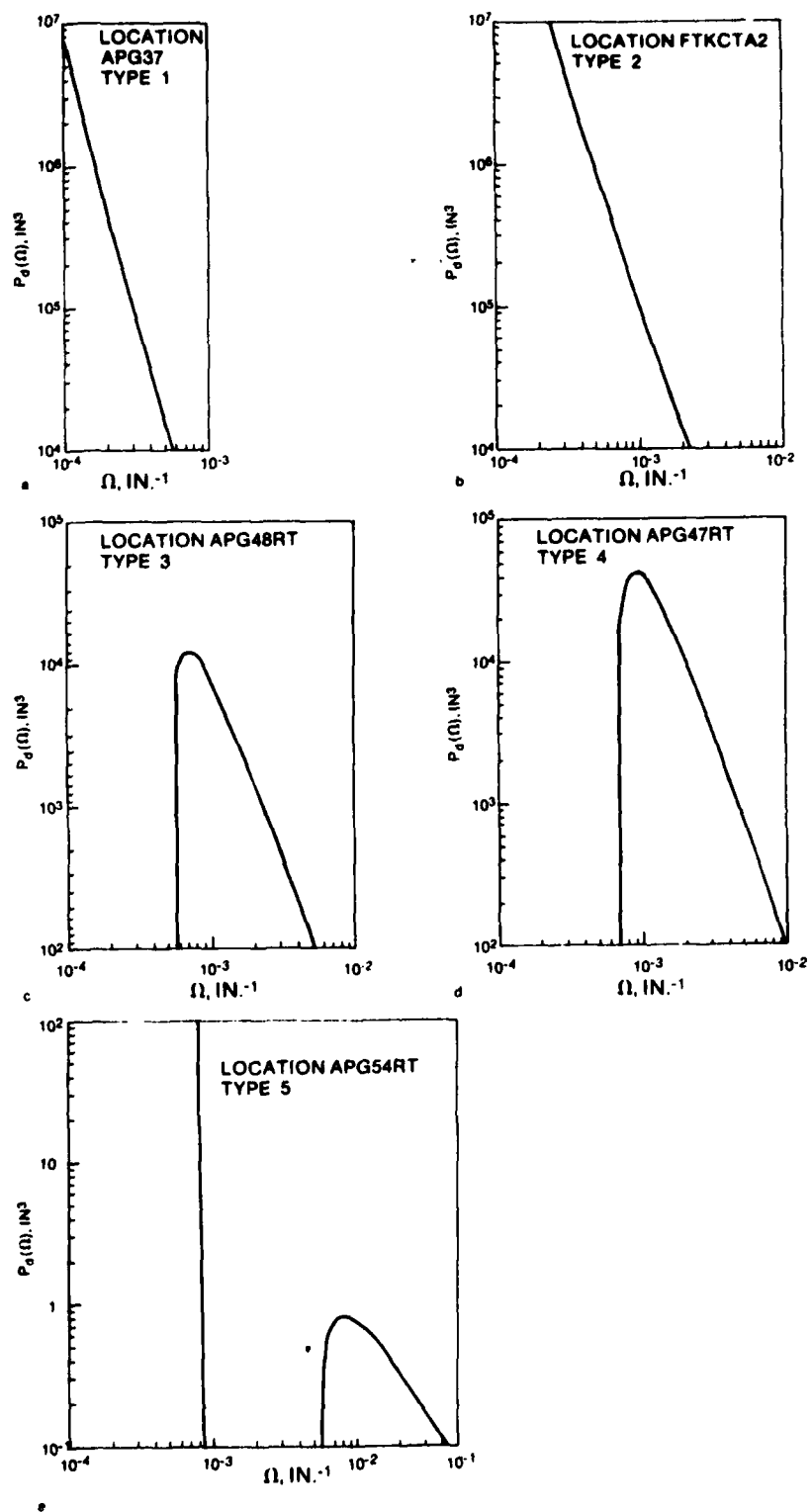


Figure 4

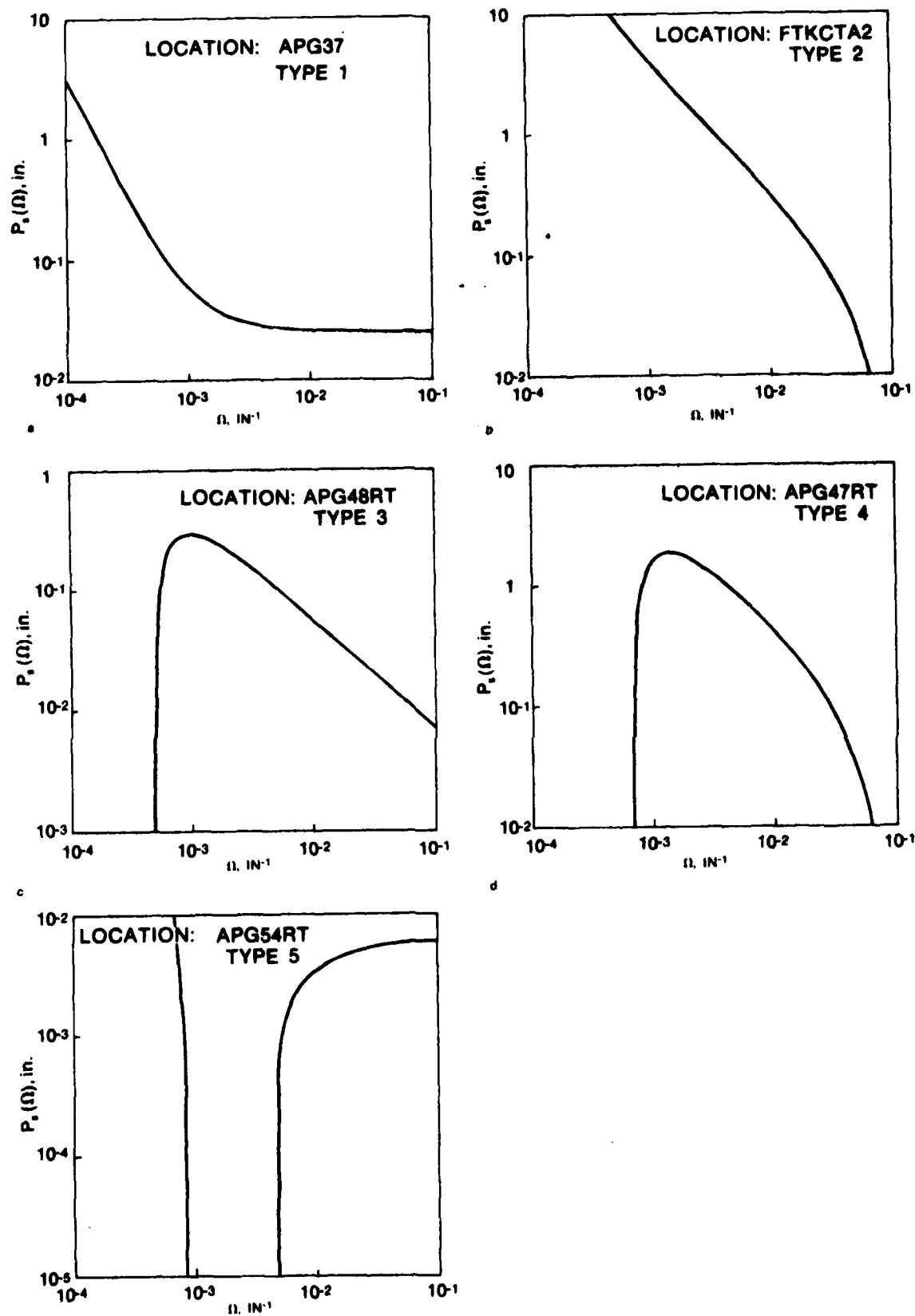


Figure 5

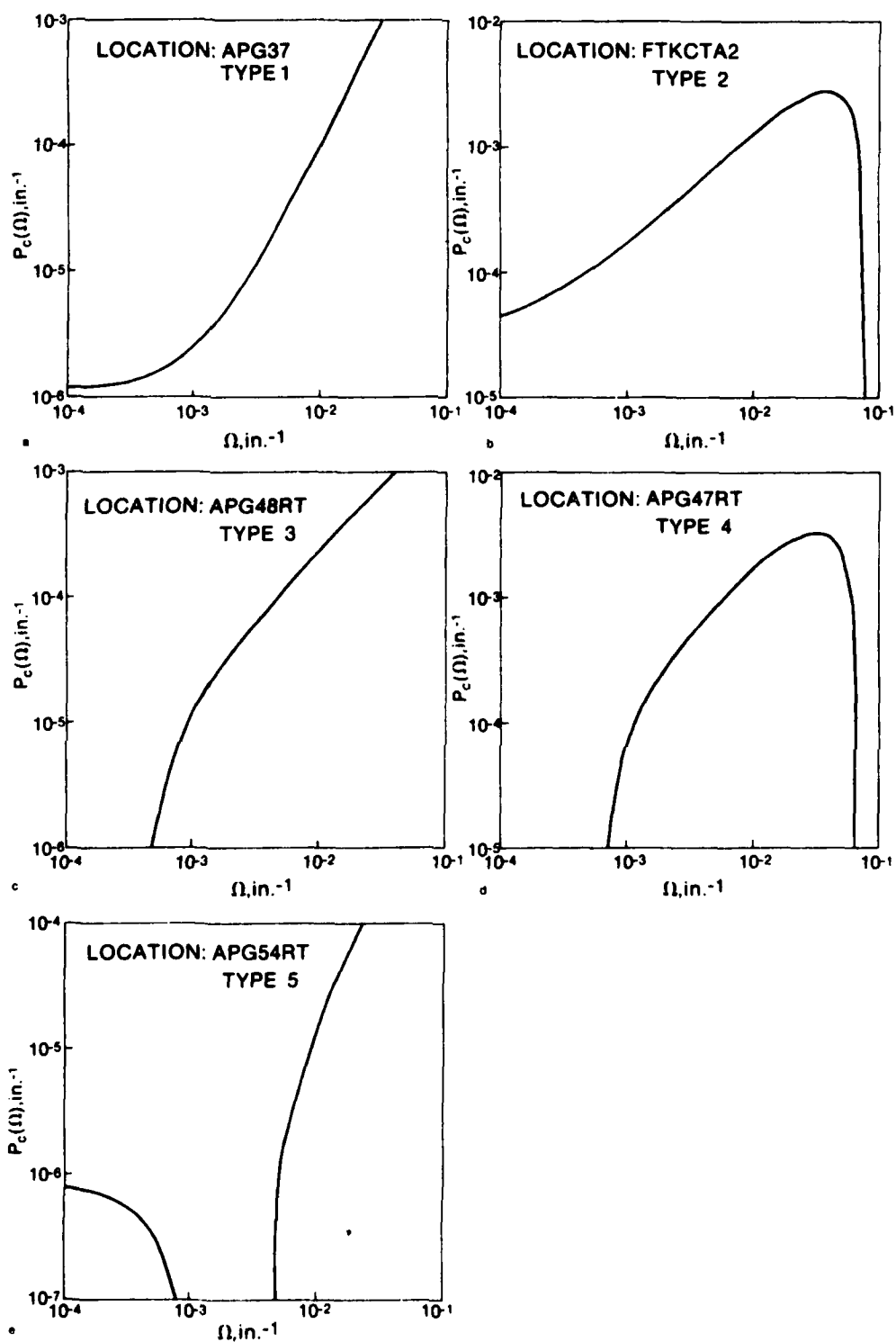
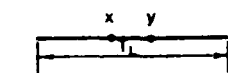
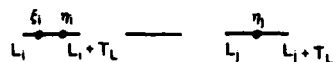
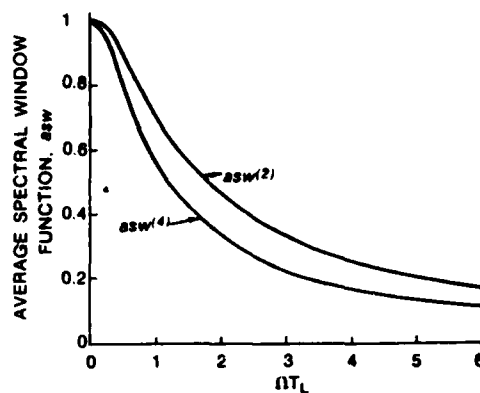


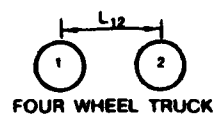
Figure 6



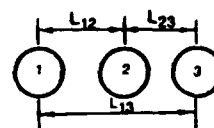
T_L = TRACK LENGTH
 x, y = INTEGRATION VARIABLES



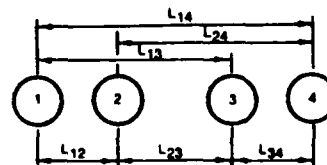
L_i = POSITION OF FRONT OF i th TIRE PRINT
 T_L = LENGTH OF TIRE PRINT
 ξ_i, η_i = INTEGRATION VARIABLES FOR i th TIRE



FOUR WHEEL TRUCK



SIX WHEEL TRUCK



EIGHT WHEEL TRUCK

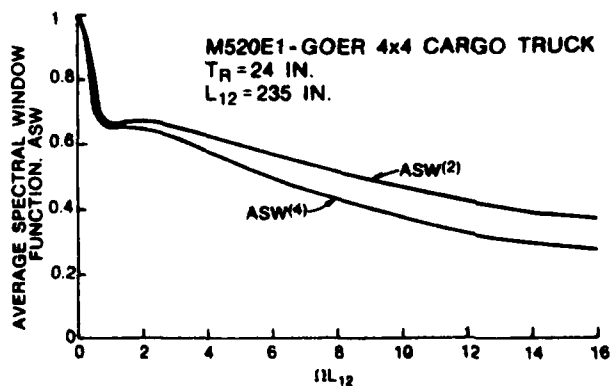


Figure 7

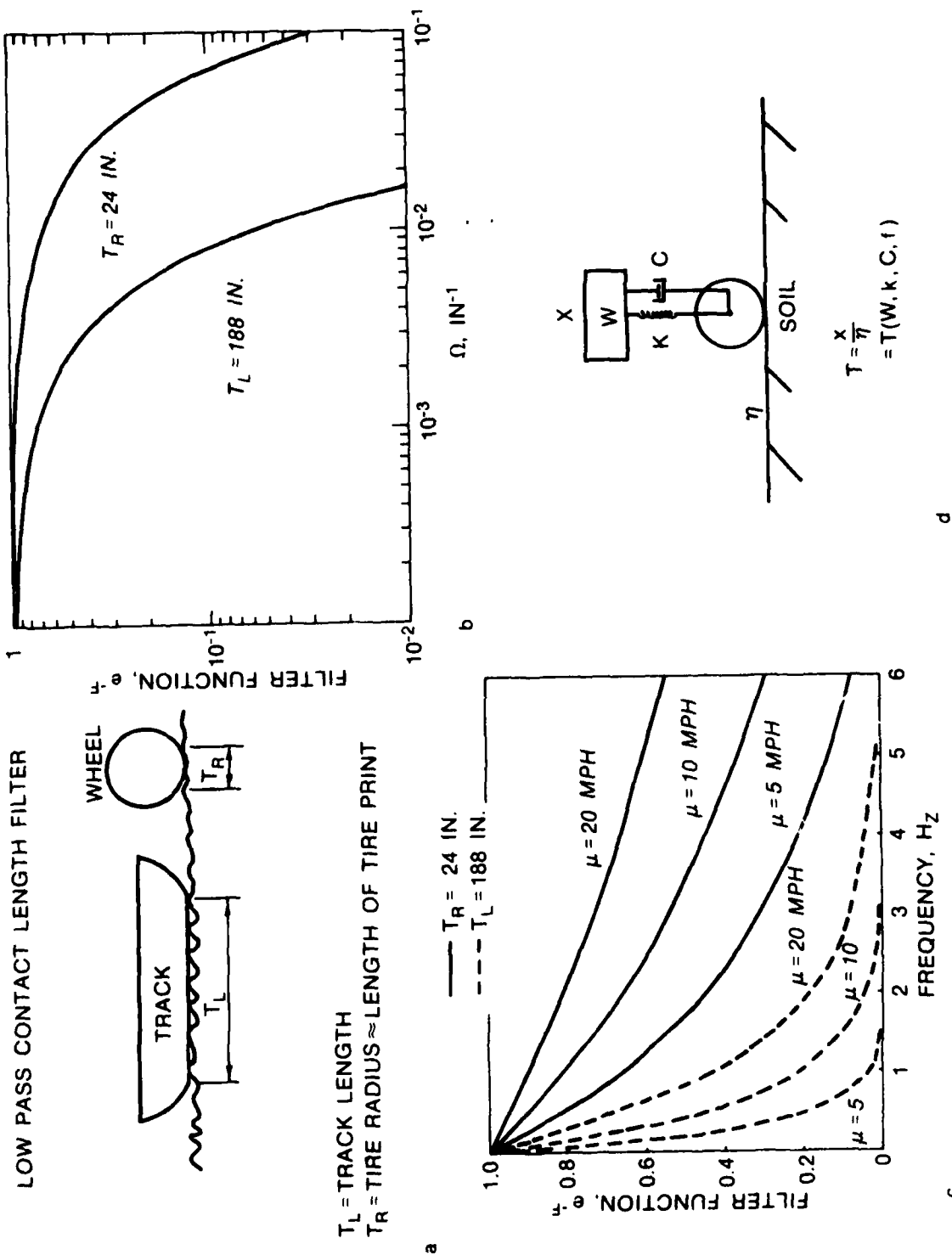
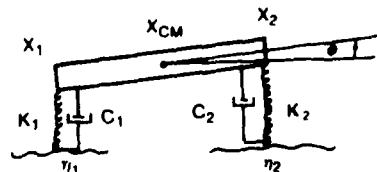
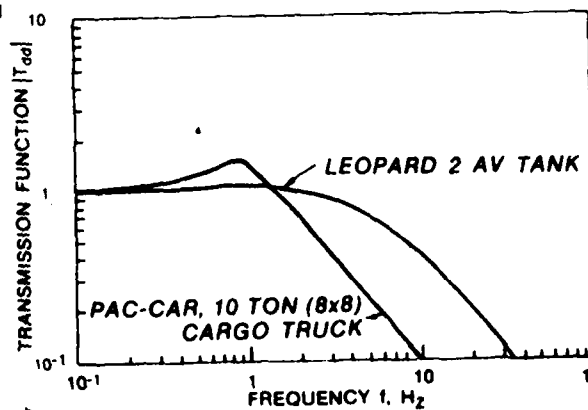
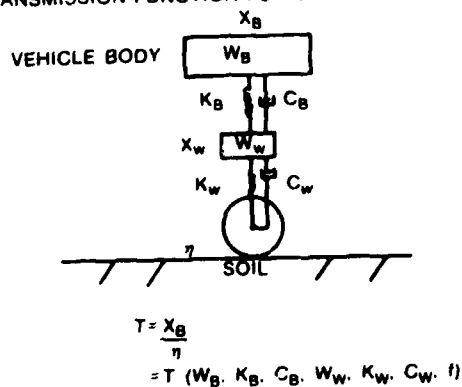


Figure 8

TRANSMISSION FUNCTION FOR VERTICAL MOTION



SOLUTION OF COUPLED DIFFERENTIAL EQUATIONS GIVES TRANSMISSION FUNCTION

$$T = \frac{X}{\eta_1} = T(M, I, K_1, C_1, K_2, C_2, f)$$

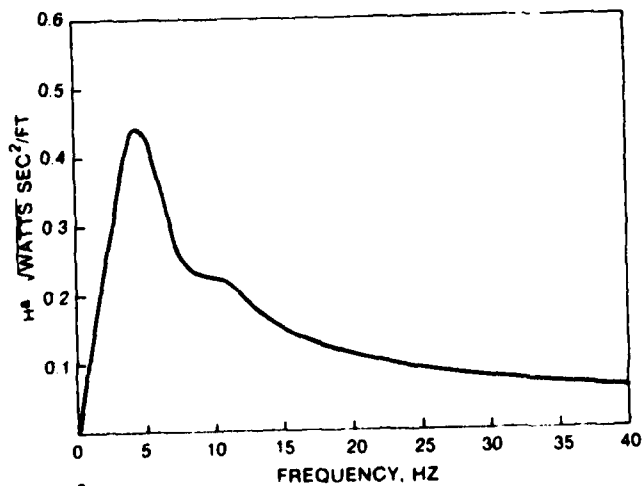
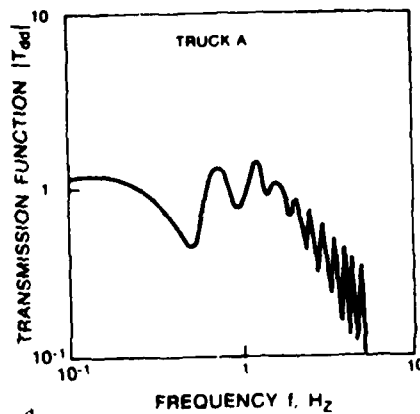


Figure 9

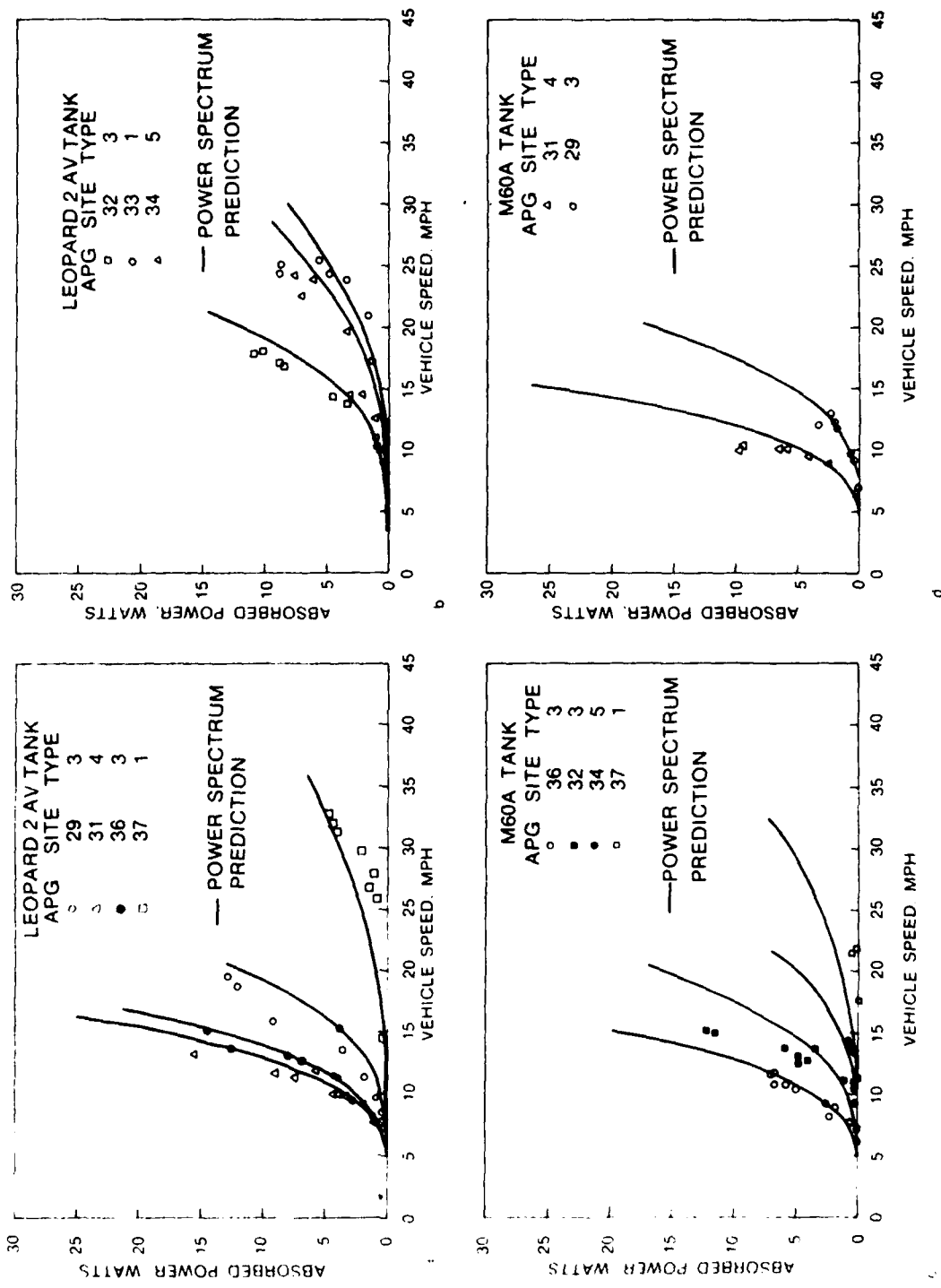


Figure 10

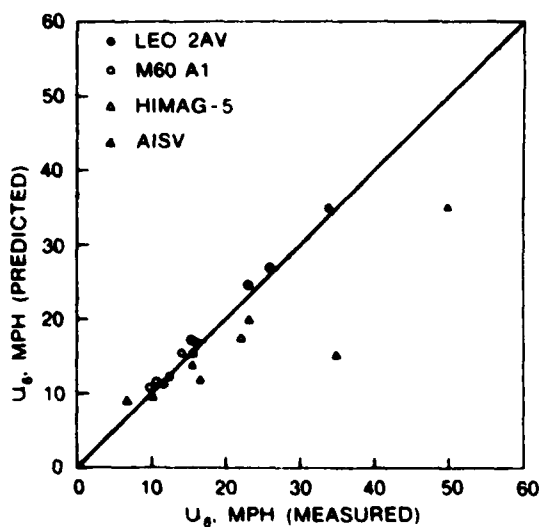
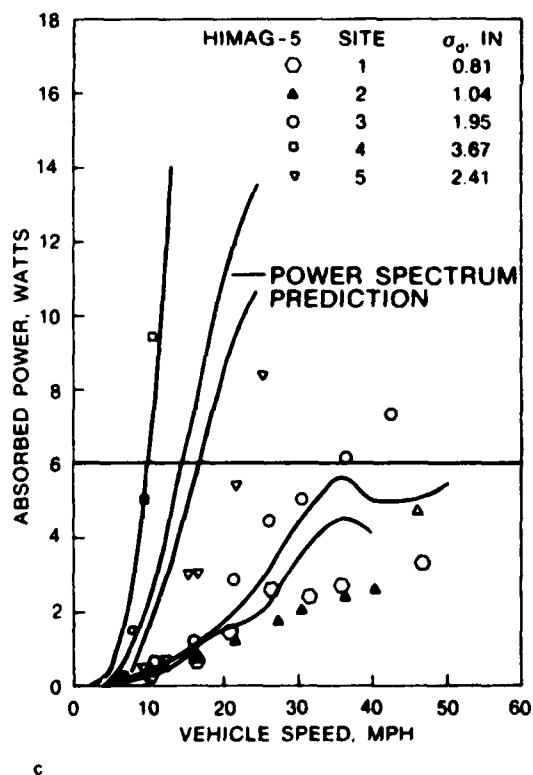
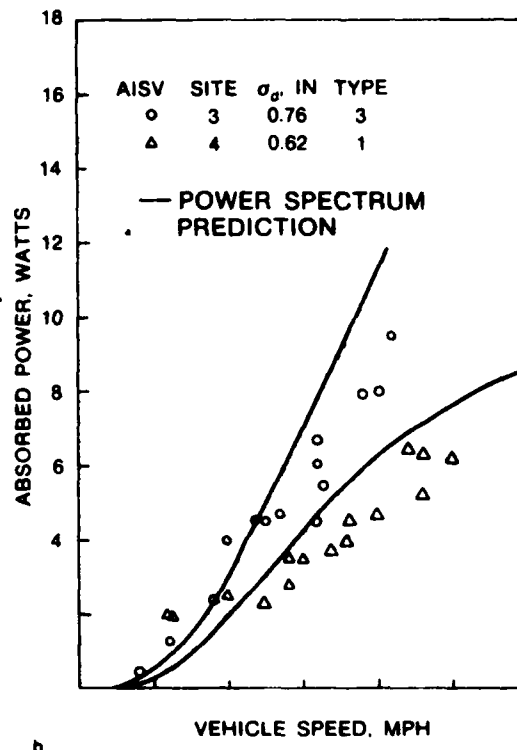
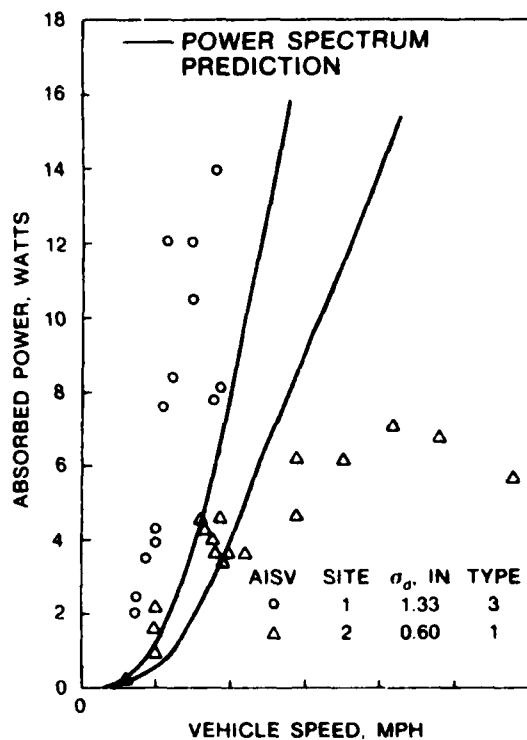


Figure 11

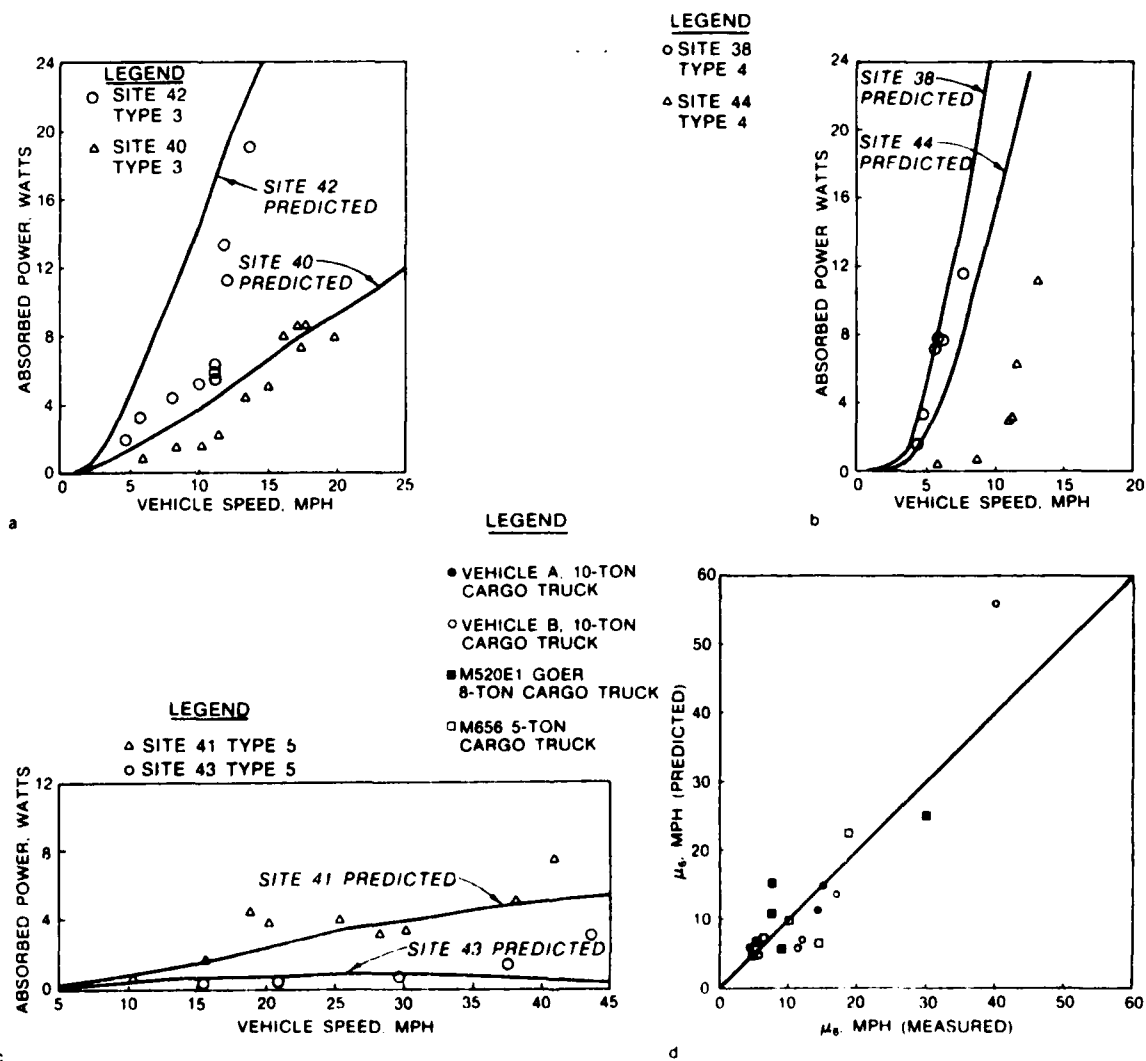


Figure 12

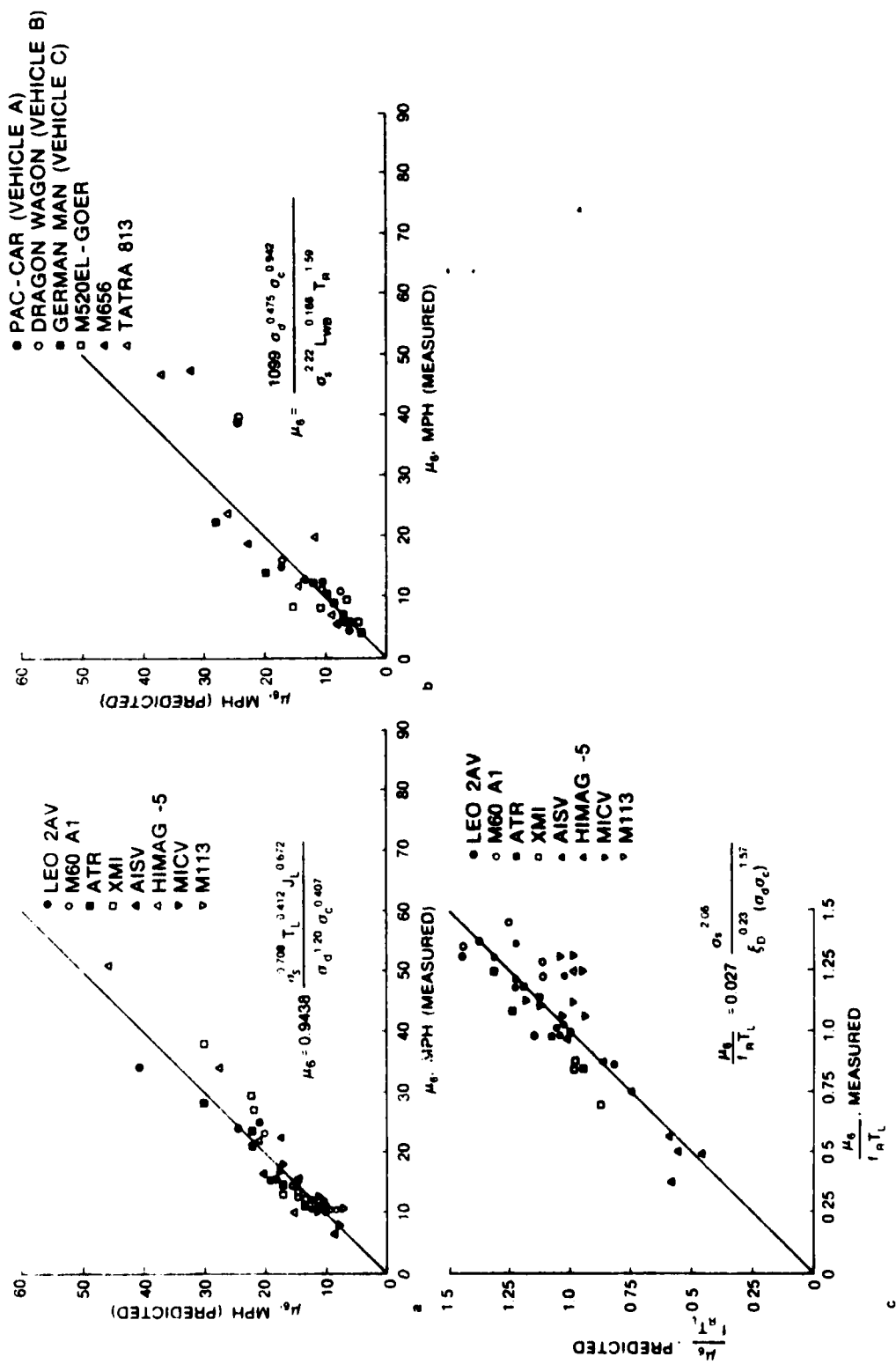


Figure 13

